DETERMINATION OF THE OPERATING CHARACTERISTICS OF A VARIABLE MACH NUMBER SUPERSONIC WIND TUNNEL

by

James L. Dozier

A Thesis Submitted to the Faculty of the

DEPARTMENT OF MECHANICAL ENGINEERING

In Partial Fulfillment of the Requirements
For the Degree of

MASTER OF SCIENCE

In the Graduate College

THE UNIVERSITY OF ARIZONA

1 9 6 4

STATEMENT BY AUTHOR

This thesis has been submitted in partial fulfillment of requirements for an advanced degree at the University of Arizona and is deposited in the University Library to be made available to borrowers under rules of the Library.

Brief quotations from this thesis are allowable without special permission, provided that accurate acknowledgment of source is made. Requests for permission for extended quotation from or reproduction of this manuscript in whole or in part may be granted by the head of the major department or the Dean of the Graduate College when in their judgment the proposed use of the material is in the interests of scholarship. In all other instances, however, permission must be obtained from the author.

SIGNED: James I Doyle

APPROVAL BY THESIS DIRECTOR

This thesis has been approved on the date shown below:

E K Parks — 4/21/64

E. K. PARKS
Professor of Mechanical Engineering

Date

ACKNOWLEDGMENTS

The author gratefully acknowledges the assistance given him by Professor E. K. Parks of the Department of Mechanical Engineering of the University of Arizona and Mr. Hiroshi Hashizume of the National Aeronautical Laboratory, Tokyo, Japan. Without their guidance and encouragement this paper would never have been completed.

TABLE OF CONTENTS

LIST OF ILLUSTRATIONS

LIST OF TABLES

ABSTRACT

The University of Arizona 3" x 4.75" vacuum storage drive supersonic wind tunnel is equipped with a supersonic nozzle of unique design. In contrast to more conventional wind tunnels which employ fixed-geometry nozzles designed for a specific Mach number, this tunnel is fitted with a continuously-variable Mach number supersonic nozzle which uses a flexible plate to form part of its contour. The nozzle is designed to give a minimum of mis-match between the elastic curvature of the flexible plate and the aerodynamic shape necessary to give parallel uniform flow throughout the range of M = 1.5 to M = 5.0.

This paper determines and evaluates the operating characteristics of this wind tunnel and compares them with those of wind tunnels using fixed-geometry nozzles.

The experiments conducted show that the performance of this supersonic wind tunnel compares very favorably with that of the other tunnels of more standard but less flexible design and that this type facility, due to its more varied usefulness and relatively low cost, is ideal for use in a university aerospace instructional program.

CHAPTER 1

INTRODUCTION

Many different types of supersonic wind tunnels have been constructed. The design and principles of operation of each are largely dependent upon the power available, test section size required, test section Mach number to be attained, and the type of testing to be undertaken. One of the more simple designs is the intermittent flow or suckdown type which is operated with a vacuum storage vessel. In this type tunnel, air at local atmospheric pressure, density, and temperature is drawn through a contraction section nozzle, test section, diffuser, and into a large evacuated storage vessel. The pressure ration available to drive the air through the circuit in this type tunnel is a direct function of the degree of vacuum which can be attained in the evacuated vessel. The advantages of this type facility are its simplicity, relatively low construction cost, and the fact that the upstream stagnation or reservoir conditions remain constant for the duration of any test run.

The most important part of any supersonic wind tunnel is the nozzle which generates the flow. The 3" x 4.75" University of Arizona tunnel is a vacuum drive suckdown type with the added feature of a continuously-variable Mach number nozzle of unique design which was initially developed by the

Arnold Engineering Development Center in Tullahoma, Alabama. Most supersonic nozzles have a curvature of fixed geometry from the nozzle throat to the test section, designed so that flow in the test section is parallel and uniform. The nozzle used on this particular tunnel, designed by the Boeing Airplane Company,[8] uses an end-supported flexible plate to form part of its variable contour and is designed to give a minimum of mismatch between the elastic curvature of the plate and the proper aerodynamic shape necessary to give parallel uniform flow throughout the Mach number range of 1.5 to 5.0.

The nozzle coordinates, flexible plate length, and pivot point location are given in Table 1.1 for a 5" test section. These coordinates, which include no boundary layer corrections can be readily converted to any other size by the use of simple similarity relationships. Figure 1.1 shows a sketch of the nozzle and defines the stages of flow generation along the nozzle as given in Table 1.1. A nozzle of this type provides a much greater degree of flexibility in the operation of the tunnel than fixed geometry nozzle blocks and greater simplicity of operation than multiple jack type variable geometry nozzles. The overall layout of the University of Arizona 3" x 4.75" supersonic wind tunnel is shown in Figure 1.2. Figure 1.3 shows the actual installation. The Schlieren camera is in the foreground. A view of the tunnel with the side plates removed to show the variable Mach number nozzle and variable geometry diffuser is shown in Figure 1.4.

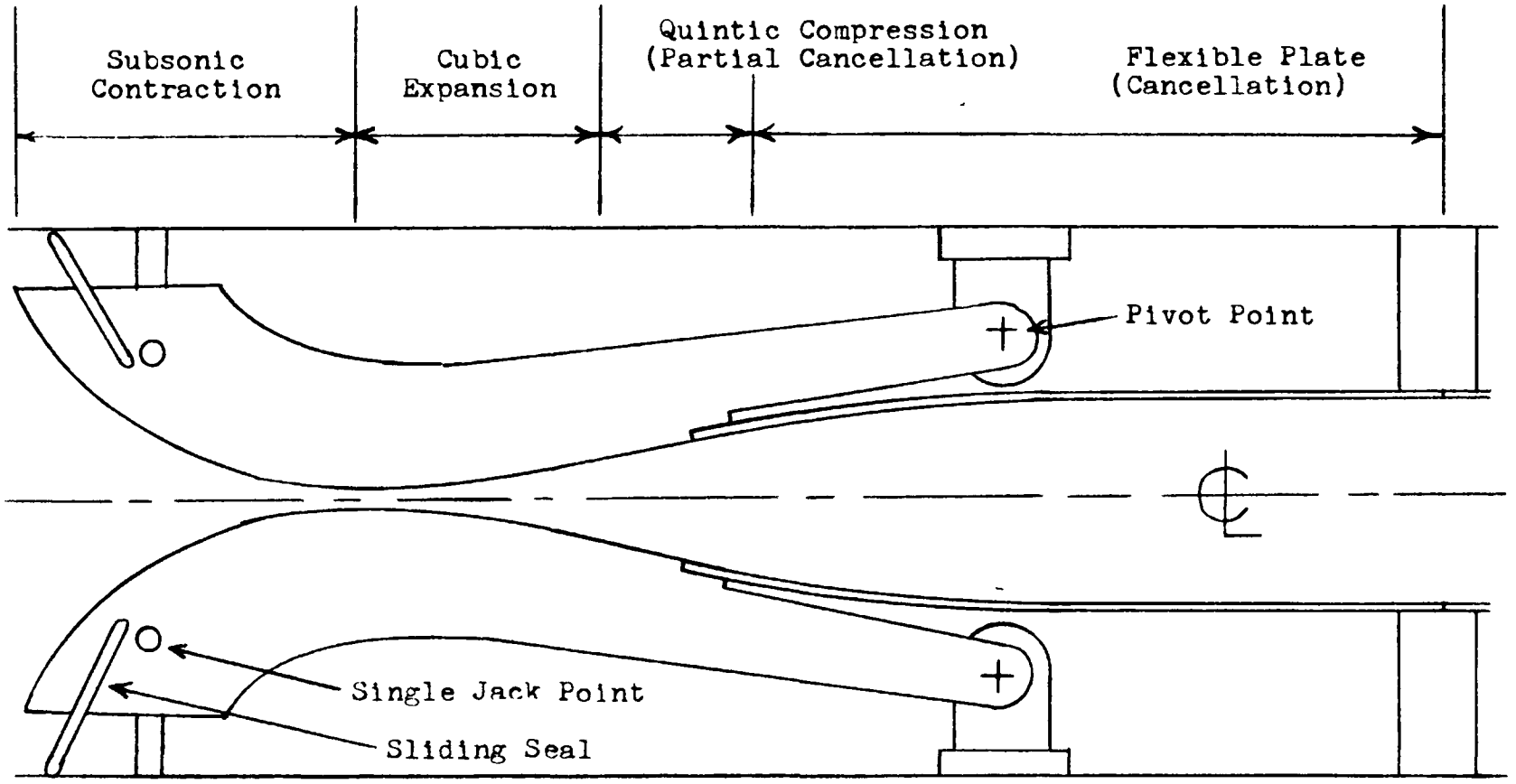

Figure 1.1 Flexible Plate Type Variable Mach Number Nozzle-Set at M = 5.0

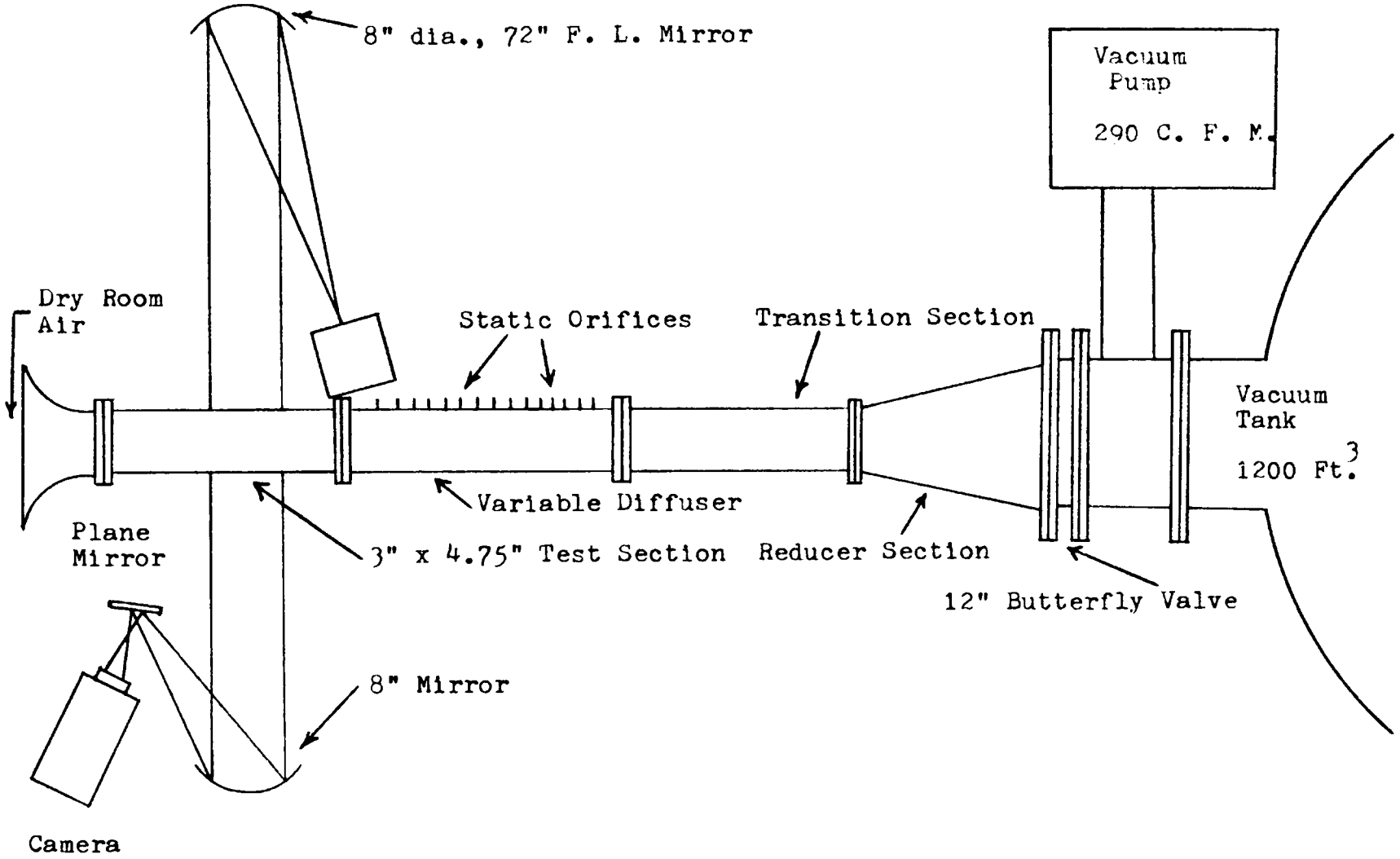

Figure 1.2 3" x 4.75" Variable Mach Number Supersonic Wind Tunnel

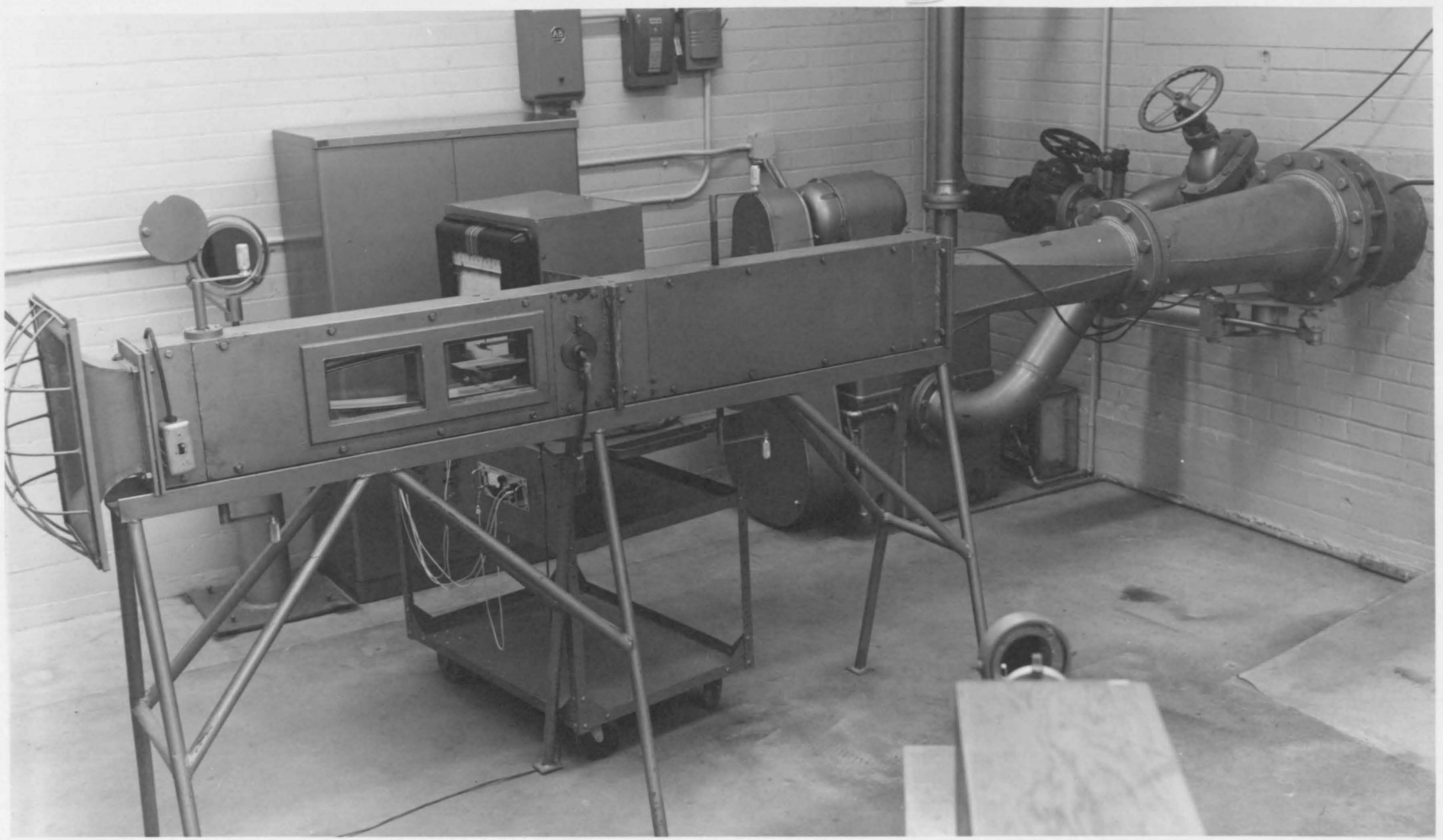

Figure 1.3 University of Arizona 3" x 4.75" Supersonic Wind Tunnel

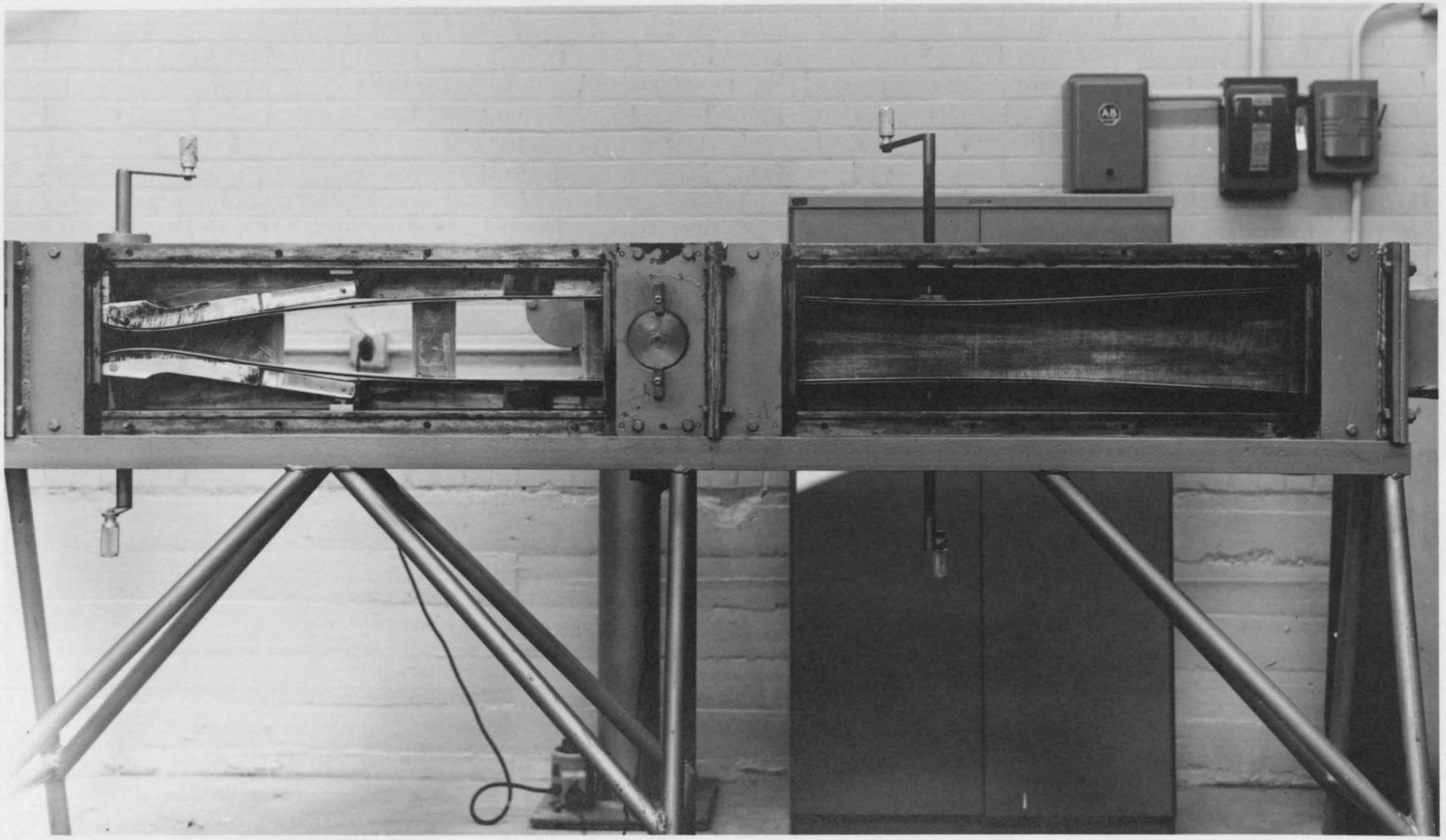

Figure 1.4 Side View of Tunnel With Side Plates Removed to Show Nozzle and Diffuser

TABLE 1.1

NOZZLE COORDINATES AT M = 5.119

The following coordinates define the rigid-section contour of a five inch supersonic nozzle in the Mach 5.119 position. There has been no correction for the boundary layer.

x	y	
-8.500	+4.6500	
	Straight Line	
-5.500	2.2450	
-5.000	1.8500	
-4.500	1.4700	
-4.000	1.1375	Subsonic Contraction
-3.500	0.8525	
-3.000	0.6200	
-2.500	0.4375	
-2.000	0.3025	
-1.500	0.1950	
-1.000	0.1275	
-0.500	0.0950	
0.000	0.0910	Sonic Throat
+0.500	0.0995	
1.000	0.1240	
1.500	0.1628	
2.000	0.2145	
2.500	0.2774	Cubic Expansion
3.000	0.3499	(Radial Flow at Exit)
3.500	0.4305	
4.000	0.5175	
4.500	0.6094	
5.000	0.7045	
5.537	0.8175	Inflection Point
6.000	0.9062	
6.500	1.001	
7.000	1.089	Quintic Compression
7.500	1.174	(Partial Cancellation)
8.000	1.258	
8.477	1.338	End of Rigid Section
		Flexible Plate

For $0 \leq x \leq 5.537$

$$y = 0.09098 + 3.511 \times 10^{-2} x^2 - 2.114 \times 10^{-3} x^3$$

and for $5.537 \leq x \leq 8.477$

$$y = 11.4268 - 8.5783x + 2.5901x^2 - 3.7612x10^{-1}x^3 + 2.6895x10^{-2}x^4 - 7.5982x10^{-4}x^5$$

For the flexible plate the ordinates are found from

$$y = 2.5 - \left[0.3453 \left(\frac{\xi}{\ell}\right)^2 + 0.8248 \left(\frac{\xi}{\ell}\right)^3\right]$$

where

$\ell = 19.980"$ and $\xi = 28.46-x$, or

$$\frac{\xi}{\ell} = \frac{28.46 - x}{19.980} \quad \text{with } 8.477 \leq x \leq 28.46$$

The pivot point coordinates for rotation of the rigid section are $x = 15.40"$, $y = 3.750"$.

CHAPTER 2

SUPERSONIC WIND TUNNEL OPERATING CHARACTERISTICS

2.1 Tunnel Running Time

In an intermittent flow vacuum storage drive supersonic wind tunnel, the flow ceases to be supersonic when the pressure in the vacuum vessel reaches a certain critical value, denoted here by p_f, which depends upon the inlet stagnation pressure p_o and the losses in the nozzle-diffuser arrangement.

In order to arrive at an expression for the running time available in this type tunnel, the changes of state in the vacuum storage vessel must first be considered. At the beginning of tunnel operation, it is assumed that the vacuum pump is turned off and that the conditions at various sections of the tunnel are as shown in Figure 2.1.

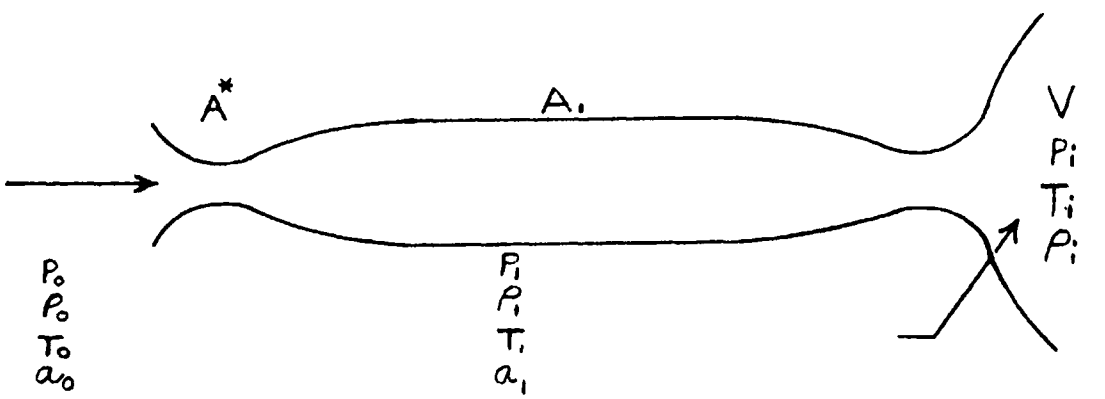

Figure 2.1 Vacuum Storage Drive Supersonic Wind Tunnel

Conditions at the end of supersonic flow are denoted by the subscript f, initial conditions by the subscript i, and conditions at any time in between by no subscript.

At any time t, the conditions in the vacuum vessel are assumed to be in equilibrium. Thus, if V is the volume of the vacuum vessel and the initial mass of air in the vessel is

$$m_i = \rho_i V = \frac{P_i V}{R T_i} \tag{2.1}$$

Let m equal the mass of air that has entered the vessel at the time t. The mass of air in the vessel at time t is therefore

$$m_i + m = \rho V = \frac{P V}{R T} \tag{2.2}$$

As long as the flow at the nozzle throat is sonic, the rate of mass flow m in the tunnel remains a constant. Hence in time interval dt, a mass of air dm flows into the vessel where

$$dm = \dot{m}\, dt \tag{2.3}$$

and the change in the density is

$$d\rho = \frac{\dot{m}}{V}\, dt \tag{2.4}$$

At time t, the density of the air in the vessel is given by

$$\rho = \rho_i + \frac{\dot{m}}{V} t \tag{2.5}$$

Relation (2.5) shows that the air density in the vacuum vessel increases linearly with time as long as the flow at the nozzle throat is sonic.

If the entire process, including the wind tunnel, diffuser, and vacuum tank, is assumed to be adiabatic, the equilibrium temperature T in the vessel at time t can be determined by equating the work done on the mass of air m flowing through the tunnel in time t to the increase in internal energy of the mass of air in the vessel during the same period. The inlet parameters remain constant during the tunnel run, therefore the work done on the air is

$$\frac{P_0 m}{\rho} = m R T_0 \tag{2.6}$$

The initial internal energy of the mass of air is

$$m_i c_v T_i + m c_v T_0 \tag{2.7}$$

The first term represents the initial internal energy of the air in the vacuum tank and the second term, the initial internal energy of the mass of air that will have flowed through the tunnel at time t. The internal energy of the total mass of air in the vessel at time t is

$$(m_i + m) c_v T \tag{2.8}$$

Applying the first law of thermodynamics and assuming the entire process to be adiabatic, relation (2.6) is equated to relations (2.7) and (2.8) to obtain

$$m R T_o = (m_i + m) c_v T - m c_v T_o - m_i c_v T_i \tag{2.9}$$

Since $R = (\gamma - 1) c_v$, relation (2.9) reduces to

$$\gamma m T_o = (m_i + m) T - m_i T_i \tag{2.10}$$

Using relation (2.3) and putting $t_i = 0$, relation (2.10) may be solved to obtain the equilibrium temperature T at any time t which gives

$$T = \frac{\gamma \dot{m} T_o t + m_i T_i}{m_i + \dot{m} t} \tag{2.11}$$

The pressure p in the vacuum vessel at time t becomes

$$P = \rho R T = \rho R \frac{\gamma \dot{m} T_o t + m_i T_i}{m_i + \dot{m} t} \tag{2.12}$$

and, using relation (2.1) and (2.2) this reduces to

$$P = P_i + \frac{\gamma \dot{m} R T_o t}{V} \tag{2.13}$$

The pressure in the vacuum vessel is therefore also seen to increase linearly with time if sonic conditions prevail at the nozzle throat. At time $t = t_f$, the pressure p_f is given by

$$P_f = P_i + \frac{\gamma \dot{m} R T_o t_f}{V} \tag{2.14}$$

By dividing both sides of relation (2.14) by p_o and solving for t_f, the running time or t_f is

$$t_f = \frac{V p_o}{\gamma \dot{m} R T_o}\left(\frac{p_f}{p_o} - \frac{p_i}{p_o}\right) \tag{2.15}$$

Using the relations[10]

$$P = \rho R T \tag{2.16}$$

and

$$\dot{m} = \rho_1 u_1 A_1 = A_1\left\{\frac{2\gamma}{\gamma-1} p_o \rho_o \left(\frac{p_1}{p_o}\right)^{\frac{2}{\gamma}}\left[1 - \left(\frac{p_1}{p_o}\right)^{\frac{\gamma-1}{\gamma}}\right]\right\}^{\frac{1}{2}} \tag{2.17}$$

where u_1 equals the test section velocity, relation (2.15) can be put into the more usable form of

$$t_f = \frac{V}{a_o \gamma A_1 M_1}\left(1 + \frac{\gamma-1}{2} M_1^2\right)^{\frac{\gamma+1}{2(\gamma-1)}}\left(\frac{p_f}{p_o} - \frac{p_i}{p_o}\right) \tag{2.18}$$

The relation $\frac{p_f}{p_o}$ is usually assumed to be $\frac{p_{o3}}{p_o}$, the pressure ratio required to maintain supersonic flow in the test section which is actually the stagnation pressure ratio across a normal shock, and it is dependent primarily on the test section Mach number and the diffuser efficiency. The ratio $\frac{p_{o3}}{p_o}$ is used to predict the theoretical running time, whereas in practice, the ratio $\frac{p_f}{p_o}$ is considerably less due to losses in the diffuser. P_f would be measured stagnation pressure in the vacuum tank at the breakdown of supersonic flow..

2.2 Effect of a Diffuser On Tunnel Running Time

The diffuser section of a supersonic wind tunnel serves the purpose of decelerating the supersonic flow developed in the test section back to subsonic velocities at its exit and to recover as much stagnation pressure as possible.

Theoretically, supersonic flows can be decelerated either isentropically or non-isentropically. Isentropic supersonic flow deceleration can be accomplished however only if the streamlines can be made to converge, therefore the flow must pass through a convergent-divergent channel. Any convergence however results in infinitesimal compression waves which coalesce to form compression or shock waves, which prevent this method of deceleration from being entirely isentropic. Supersonic flows can also be decelerated through a system of shock waves in an entirely non-isentropic process which results in large stagnation pressure losses.

An ideal supersonic diffuser is one in which no shock losses at all occur; the flow outside of the boundary layer being decelerated isentropically from the design supersonic speed at the diffuser entrance section to the speed of sound again at the diffuser throat. Downstream of the diffuser throat the flow undergoes further deceleration in the divergent or subsonic part of the diffuser. This is the reverse of the process that takes place in the supersonic nozzle. Theoretically these two nozzles could be mirror images of each other.

An ideal diffuser can never be realized in practice however, for several reasons. One is due to the fact that the boundary layer tends to separate from the diffuser walls because of the unfavorable pressure gradient in the convergent part of the diffuser. This separation produces a system of weak oblique shocks in the contraction section of the diffuser. In addition, the diffuser throat must be larger in area than the nozzle throat in order to establish supersonic flow in the test section, although variable diffusers can approach this equality of area ratios by decreasing the area of the second throat once supersonic flow has been established. Finally, experience[5] has shown that the only stable position for a normal shock in the diffuser is downstream of the diffuser throat, which also means that the flow is not entirely isentropic.

All of these deviations from isentropic flow result in stagnation pressure losses. These losses are smaller, nevertheless, in a properly designed convergent-divergent diffuser than they would be in a simple straight through diffuser, one in which deceleration of the flow is accomplished entirely through a system of shock waves. Further improvement in pressure recovery can be made if the diffuser throat can be closed somewhat once supersonic flow has been established in the manner previously mentioned. This is quite difficult to do without an elaborate system of controls in an intermittent flow supersonic wind tunnel due to the short duration of the running time. The most practical

diffuser arrangement for this type tunnel is a fixed convergent-divergent type second throat. The University of Arizona 3" x 4.75" supersonic wind tunnel has this type diffuser. It is constructed similarly to the supersonic nozzle in that it utilizes flexible plates to form its contour. It is thus possible to vary the diffuser opening while at the same time maintaining the nozzle contours necessary to provide a minimum of boundary layer separation as the flow decelerates. As will be shown, this type diffuser does provide some increase in the available tunnel running time.

2.3 Diffuser Efficiency

A number of relationships have been formulated or suggested to define the efficiency of a supersonic diffuser. One of the more widely accepted ones[5] defines the diffuser efficiency as the work of isentropic compression between the test section or diffuser entrance conditions, p_1, M_1, T_1, as shown in Figure 2.1, and the final conditions, p_3, M_3, and T_3, at the diffuser exit section divided by the kinetic energy expended, i.e., the efficiency is defined as the ratio of the isentropic increase in the enthalpy between the entrance and exit of the diffuser to the change in kinetic energy in the diffuser.

The isentropic increase in enthalpy is given by

$$C_p(T_3 - T_1) = C_p T_1 \left(\frac{T_3}{T_1} - 1\right) \tag{2.19}$$

or, using relation (2.16) and

$$\frac{P}{P_0} = \left(\frac{\rho}{\rho_0}\right)^{\gamma} \tag{2.20}$$

$$c_p(T_3 - T_1) = c_p T_1 \left[\left(\frac{P_3}{P_1}\right)^{\frac{\gamma-1}{\gamma}} - 1\right] \tag{2.21}$$

and the change in kinetic energy per unit mass is given by

$$\frac{1}{2}\left(u_1^2 - u_3^2\right) \tag{2.22}$$

where u_3 is the flow speed at the diffuser exit section. Using relations (2.21) and (2.22), the diffuser efficiency becomes

$$\eta = \frac{c_p T_1 \left[\left(\frac{P_3}{P_1}\right)^{\frac{\gamma-1}{\gamma}} - 1\right]}{\frac{1}{2}\left(u_1^2 - u_3^2\right)} \tag{2.23}$$

However, since

$$a_1^2 = \gamma R T_1 = c_p(\gamma - 1) T_1 \tag{2.24}$$

$$\eta = \frac{\frac{2}{\gamma-1}\left[\left(\frac{P_3}{P_1}\right)^{\frac{\gamma-1}{\gamma}} - 1\right]}{M_1^2 - \frac{u_3^2}{\gamma R T_1}} \tag{2.25}$$

If u_3 is relatively small, which is the case, relation (2.24) becomes

$$\eta = \frac{2}{(\gamma-1)M_1^2}\left[\left(\frac{P_{03}}{P_1}\right)^{\frac{\gamma-1}{\gamma}} - 1\right] \tag{2.26}$$

This is a usable expression for the efficiency of a supersonic diffuser and the one used to plot the theoretical curve in Figure 5.3.

2.4 Test Section Reynolds' Number

The Reynolds' number R_e is given by

$$R_e = \frac{u L \rho}{\mu} \tag{2.27}$$

where L is a significant dimensional parameter of the model. Experiments have shown[5] that the coefficient of viscosity is independent of pressure in the range of .001 - 20 atmospheres and that an empirical relationship known as Sutherland's formula

$$\frac{\mu}{\mu_0} = \frac{T_0 + 216}{T + 216}\left(\frac{T}{T_0}\right)^{\frac{3}{2}} \tag{2.28}$$

best represents the variations of the coefficient of viscosity relative to temperature, with the temperatures in degrees Rankine.

If μ is based on Sutherland's formula and the relations (2.16), (2.24), (2.27) and the isentropic relation

$$\frac{\rho}{\rho_0} = \left(\frac{T}{T_0}\right)^{\frac{1}{\gamma-1}} \tag{2.29}$$

are used, the "free stream" Reynolds' number per unit length becomes

$$\frac{R_e}{L} = \frac{P_o M_1}{\mu_o}\left(\frac{\gamma}{RT_o}\right)^{\frac{1}{2}}\left(\frac{T_o}{T_1}\right)^{\frac{\gamma-2}{\gamma-1}}\left(\frac{T_1+216}{T_o+216}\right) \qquad (2.30)$$

This expression is especially applicable to the intermittent flow vacuum storage drive tunnel in that the stagnation conditions remain constant during the tunnel run.

2.5 Mach Number Measurements

The Mach number in supersonic flow may be calculated from several pressure relationships, however if isentropic flow is assumed in the nozzle and test section, the relation[4]

$$\frac{P_1}{P_o} = \left(1 + \frac{\gamma-1}{2}M_1^2\right)^{\frac{\gamma}{\gamma-1}} \qquad (2.31)$$

is most convenient to use on the tunnel being investigated. The assumption of isentropic flow is valid in that the air passing through the supersonic nozzle undergoes a continuous expansion in the divergent portion of the nozzle and if the nozzle is correctly designed, there should be no non-isentropic shock formations. Experience has shown that this is the case. The Mach number may therefore be calculated if the static pressure p_1 at a point in the flow is known. p_o is the local atmospheric pressure. The Mach number for air as a function of $\frac{P_1}{P_o}$ is tabulated in Reference 1 which was used in these experiments.

2.6 Boundary Layer Corrections

The flow field in a supersonic channel is considered as consisting of a central core of non-viscous or potential flow surrounded by a layer of retarded or viscous flow along the channel walls called the boundary layer. Conventional methods of supersonic nozzle design are based on the assumption that the effects of boundary layer growth can be accounted for by a correction of the potential flow contours.

The most convenient method of supersonic nozzle contour corrections to compensate for the effects of boundary layer growth is based on the boundary layer displacement thickness δ^*. The displacement thickness has the physical significance that the retardation in the mass flow through the boundary layer is equivalent to an inward shift or displacement of the contoured wall by the amount δ^*.

For most cases, the exception being extremely small wind tunnels, the Reynolds' number downstream of the nozzle throat is greater than the transition Reynolds' number, therefore the boundary layer downstream is fully turbulent. In computing the boundary layer corrections it is customary to neglect the boundary layer displacement thickness at the nozzle throat and to assume that the effective origin of boundary layer growth is the nozzle throat itself. The boundary layer "corner effect" is also neglected in computing two-dimensional boundary layers. The radius of the boundary layer fillet in the corner of a two-dimensional channel has been found to be of the order of the boundary

layer thickness. Since optical flow measuring techniques are usually used on supersonic wind tunnels, the boundary layer corrections for the nozzle are applied only to the upper and lower nozzle contours and not to the side walls which are designed to remain parallel. Even with the side wall remaining parallel, the flow will remain essentially two-dimensional for most cases.

An empirical expression for the growth of the displacement thickness boundary layer can be obtained by first considering the von Karman momentum integral equation for compressible flow along a flat plate which is

$$\frac{d}{dx}\left(\bar{\rho}\bar{u}^2\Theta\right) + \bar{\rho}\bar{u}\,\delta^*\frac{d\bar{u}}{dx} = \tau_o \tag{2.32}$$

where the bar indicates values at the outer edge of the boundary layer. If a zero pressure gradient is assumed, relation (2.32) becomes

$$\frac{d\Theta}{dx} = \frac{\tau_o}{\bar{\rho}\bar{u}^2} \tag{2.33}$$

Experimental data[8] has shown that the most suitable expression for the local skin friction coefficient is

$$\frac{c_f}{2} = \frac{\tau_o}{\rho_w \bar{u}^2} = .0131\left(\frac{\nu_w}{\bar{u}x}\right)^{\frac{1}{7}} \tag{2.34}$$

where the subscript w indicates wall values. Using relation (2.34), relation (2.33) becomes

$$\frac{d\Theta}{dx} = .0131\left(\frac{\nu_w}{\bar{u}x}\right)^{\frac{1}{7}} \tag{2.35}$$

Direct integration yields

$$\Theta = (.0131)\left(\frac{7}{6}\right)\left(\frac{\sqrt{\tau_w}}{\bar{u}}\right)^{\frac{1}{7}} X^{\frac{6}{7}} \tag{2.36}$$

which simplifies to

$$\Theta = .01528\left(\frac{\sqrt{\tau_w}}{\bar{u}\,X}\right)^{\frac{1}{7}} \tag{2.37}$$

which is an expression for the momentum thickness of the boundary layer. Reference 7 gives a relationship between δ^* and Θ relative to the test section Mach number, which is

$$\frac{\delta^*}{\Theta} = \text{boundary layer shape factor}$$

From this relationship, δ^* can be computed. Ruptash[8] further refined this method on the basis of experimental data to arrive at an empirical expression for the growth of δ^* as a function of the Mach number which is

$$\delta^* = \frac{1}{67}\left(\frac{\sqrt{\tau_w}}{\bar{u}_1 X_1}\right)^{.14} M_1^{.75} X \tag{2.38}$$

The relationships used to compute the boundary layer corrections for the University of Arizona supersonic wind tunnel are

(1) $\delta^* = \frac{1}{67}\left(\frac{\sqrt{\tau_w}}{\bar{u}_1 X}\right)^{.14} M_1^{.75} X$ Reference 8

(2) $T_w = T_1\left(1 + r\frac{\gamma-1}{2}M_1^2\right)$ Reference 7

(3) $r = \sqrt[3]{P_r}$ Reference 7

(4) $\sqrt{\tau_w} = \frac{\mu_w}{\rho_w}$ Reference 7

$$(5)\quad \frac{\mu_w}{\mu_o} = \left(\frac{T_w}{T_o}\right)^{\frac{3}{2}} \frac{T_o + 216}{T_w + 216} \qquad \text{Reference 7}$$

Equation (3) is used to compute the temperature recovery factor r, which is used to compute T_w. T_w was substituted into equation (4) to arrive at a value for μ_w. Equations (5) and (1) were then used to compute the theoretical values of δ^*. T_o is the atmospheric temperature at the time of the tunnel run. T_1, u_1, and ρ_1 were obtained from Reference 1. The values of x and x_1 were taken as 21 inches, the distance from the nozzle throat to the center of the test section.

CHAPTER 3

TUNNEL INSTRUMENTATION

3.1 Description of Instrumentation

The University of Arizona 3" x 4.75" supersonic wind tunnel has a variety of equipment available for flow instrumentation. The Schlieren apparatus has already been mentioned in Figure 1.2, but its versatility should be amplified a bit. Its screen assembly is equipped with a shutter and lens that permit the use of still photography. Both Polaroid and standard pictures have been made with this setup with a great deal of success. Highspeed movies have been made of images on the screen itself with satisfactory results. In addition, the knife edges can be utilized either vertically or horizontally. The entire Schlieren assembly may be easily removed from the tunnel for use elsewhere. The correct positions of the mirrors and the camera-screen assembly are marked on the laboratory floor and require only fine adjustments when they are returned to the tunnel from other uses.

For pressure instrumentation, a multiple bank mercury manometer is available as well as two Statham differential pressure transducers. One transducer has a range of zero to $\pm$ 1 psid, the other a range of zero to $\pm$ 15 psid. The transducers may be attached to a Leeds and Northrup

Type G Speedomax recording potentiometer, consisting of a bridge whose output is recorded in ink on a graph paper scroll. This recorder has a variable sensitivity that permits measurements of high accuracy. The tunnel itself has removable side plates on the test section and diffuser section. One of these side plates has a horizontal series of static pressure taps one inch apart that extend from upstream of the nozzle throat to downstream of the test section. In addition it has a vertical series of taps one inch apart at the test section. There are also several types of probes available that my be mounted in the test section. The size and complexity of these probes is limited however due to the relatively small test section area. A McLeod gauge is also available for the measurement of extremely low absolute pressures. Figure 3.1 shows the recorder, McLeod gauge, transducer, and Schlieren source.

3.2 Calibration of Instrumentation Used

The experiments conducted to determine the operating characteristics of the tunnel utilized the static pressure taps along the tunnel wall, the zero $\pm$ 15 psid transducer, the Speedomax recorder, and the McLeod gauge.

The calibration procedure consisted of first standardizing the recorder by inserting a resistor into the bridge circuit in place of the transducer. This was necessary since the recorder was used for other purposes during

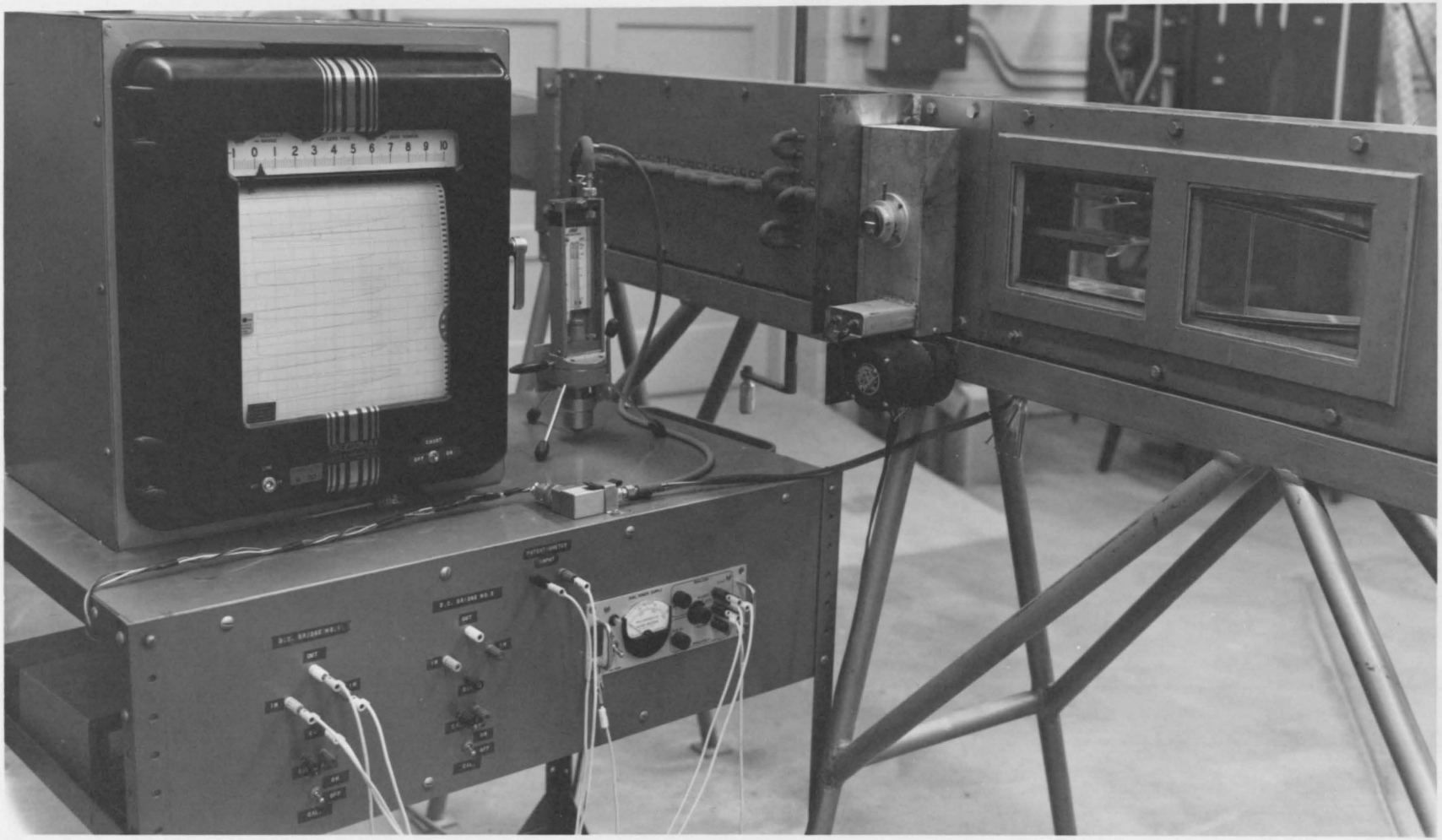

Figure 3.1 Wind Tunnel Instrumentation

the course of these experiments. This resistor would give a specific scale deflection that was used as a reference each time the recorder was used. The recorder was thus easily calibrated for each days use.

The transducer was calibrated using the McLeod gauge. A vacuum line was run from the vacuum storage vessel to a "T" connection. One side of the "T" was connected to the McLeod gauge, the other side to the transducer. The vacuum vessel was evacuated and the absolute pressure read on the McLeod gauge and a corresponding deflection read on the recorder. The scale deflection represented the millimeters of pressure differential across the transducer. Thus by subtracting the absolute pressure indicated on the McLeod gauge from the barometric pressure reading at the time, the recorder scale reading could be converted into millimeters of "vacuum". This could have been done only once and the known resistor used to calibrate the entire apparatus thereafter, but to insure accuracy, it was done prior, during, and after each series of tunnel runs. The results of this calibration showed that transducer performance was essentially linear in the absolute pressure range of 1.0 to 100 millimeters of mercury, the region where most of the readings were taken, thus a linear variation was assumed throughout. The multiple bank manometer and the pressure probes were not used.

CHAPTER 4

CONDUCT OF THE EXPERIMENTS

4.1 General

The tunnel operating characteristics to be determined consisted of the running time available at various vacuum tank pressures, Mach numbers, and diffuser settings; a Mach number traverse along the centerline of the tunnel and also a vertical traverse in the test section; a determination of the boundary layer thickness corrections to be applied to the nozzle contours, and finally the pumping time necessary to reach a given vacuum in the tank.

4.2 Tunnel Running Time

Since the running time available with this type of tunnel depends upon the initial back pressure in the vacuum tank, the Mach number, and the amount of stagnation pressure recovery attainable with the diffuser, the procedure used to determine the running time involved a variation of each of these parameters in turn.

Back pressures of 10mm and 100mm of Hg. absolute were chosen as the reference back pressures in the vacuum vessel. At a particular Mach number, two runs of the tunnel were made with each of these back pressures. One run was made with the diffuser all the way open, the other with the

diffuser set as close to the minimum starting area ratio as possible.

At this point it is appropriate to mention that the efficiency of the diffuser on this particular tunnel is reduced because of a shock formation that is produced due to a mismatch between the ends of the flexible plates that form the diffuser contours and the upper and lower walls of the test section. This mismatch of about 1/8 inch is caused by a warping of the flexible plates at the points where they are attached to the tunnel frame. To eliminate this problem the plates would have to be replaced, or at least removed and straightened. No attempt to do this was made inasmuch as the order of magnitude of the stagnation losses suffered due to this system of shock waves is considered to be of the same order as those produced by a model in the test section.

Nevertheless, the diffuser did have an appreciable effect on the running time of the tunnel as can be seen in Figure 5.2.

The duration of the flow was chosen as the time interval between the complete opening of the quick acting valve and the return of the normal shock back through the test section. The return of the normal shock could be observed visually on the Speedomax recorder. These time intervals were timed with a stopwatch and may be considered conservative in that viewing the establishment of the flow

over a model through the Schlieren shows that the flow becomes uniform within a fraction of a second of the full opening of the valve. The running time available under the various conditions imposed upon the tunnel are shown in Figure 5.2.

4.3 Diffuser Efficiency

The diffuser efficiency was computed using relation (2.26) based on the stagnation pressure readings in the vacuum storage vessel at the breakdown of supersonic flow in the test section. The results are plotted in Figure 5.3 and are based on the diffuser throat set at the minimum starting area ratio.

4.4 Mach Number Traverses

Assuming isentropic flow, the Mach number traverse along the centerline and the vertical traverse in the test section were performed by making static pressure measurements at the stations one inch apart in the tunnel wall. All of the static taps were used.

The static pressure taps were connected by a 1/8 inch inside diameter rubber hose to the zero to $\pm$ 15 psid transducer and hence to the recorder. This provided a very satisfactory method of pressure measurement at all Mach numbers. At the lower Mach numbers with their higher tunnel static pressures, the differential pressures were read directly using atmospheric pressure as a reference

with the recorder adjusted for a maximum scale deflection at minimum sensitivity. The minimum sensitivity setting was necessary in that at higher sensitivities the pointer would run off of the scale. Above a Mach number of 4.0 however, the static pressures were so low that it was difficult to observe on the recorder critical small differences in scale readings. In order to be able to measure small differences in the static pressure, atmospheric pressure was no longer used as a reference. Instead, a pressure tap well downstream of the nozzle throat was calibrated against atmospheric pressure so that it could be used as a new reference. The sensitivity of the recorder was then doubled so that smaller differences in pressure would produce full scale readings. In this manner three significant figure accuracy was maintained in the pressure traverses made at Mach number of 4.5 and 5.0.

4.5 Vacuum Vessel Pumpdown Time

The University of Arizona supersonic wind tunnel is driven by a 1200 cubic foot underground vacuum storage vessel. A Stokes Microvac pump of 290 cubic feet per minute capacity, driven by a 10 hp, 490 rpm Reuland electric motor is used to evacuate the storage vessel. The performance of this system is tabulated in Figure 5.14 based on absolute pressure readings taken from a mercury manometer during the evacuation of the storage vessel. The vacuum pump can be seen in the center background of Figure 1.3.

4.6 Boundary Layer Corrections

The method used to measure the displacement thickness of the boundary layer in the test section consisted of setting a measured area on the supersonic nozzle throat and then running the tunnel to ascertain the Mach number of the flow. The nozzle/test section area ratio was obtained from Reference 1 for the particular Mach number. The effective test section area thus obtained was compared to the actual test section area and the difference attributed to the displacement thickness of the boundary layer. A linear variation in boundary layer growth from the nozzle throat to the test section was assumed. The results obtained using this method are tabulated in Figure 5.12.

CHAPTER 5

EVALUATION OF EXPERIMENTAL RESULTS

5.1 Tunnel Running Time

The running times obtained showed that the tunnel performs extremely satisfactorily. Figure 5.3 shows the measured running times plotted versus two curves. One of the curves was obtained using the values $\frac{P_{os}}{P_o}$ from Reference 4 in the running time equation. This criterion proved to be satisfactory up to about a Mach number of 3.0 with the diffuser set at the minimum starting area ratio. A more appropriate curve was obtained using the values of $\frac{P_{os}}{P_o}$ across a normal shock. The running times at Mach number of 1.39 to 4.0 very closely approximated this curve. The effect of the diffuser on the running time is noticeable. With the diffuser set as close to the minimum starting area ratio as possible, improvements in running time of about 10%-15% were obtained. This improvement was obtained even though the previously mentioned discontinuity at the entrance to the diffuser existed. The only running times plotted in Figure 5.2 are those resulting from an initial back pressure of 10mm of mercury in the vacuum vessel. Tunnel runs of shorter duration at all but the upper Mach numbers were made at higher back pressures but were not considered to be significant to this evaluation.

5.2 Diffuser Efficiency

Diffuser efficiency for two different diffuser configurations are plotted in Figure 5.3. One curve is for a straight through diffuser and the other for a convergent-divergent fixed geometry diffuser. The efficiency based on experimental data and using relation (2.26) is also plotted and is seen to conform most closely to the straight through diffuser curve even though the diffuser was set at the minimum starting area ratio. This indicates that the expected stagnation pressure recovery with this diffuser configuration was not obtained. This can be attributed in part to the discontinuity at the diffuser entrance.

5.3 Mach Number Traverses

The horizontal and vertical Mach number traverses showed that at all except the upper two Mach numbers investigated, the flow in the test section was uniform and compares favorably with that obtained in supersonic tunnels that have fixed geometry supersonic nozzles. The test section Mach number is uniform up to about two inches from the rear of the test section. At this point the Mach number tends to drop off. This is not considered a drawback however, as all models used in the tunnel are mounted well forward of this position.

At Mach numbers between 4.0 and 5.0 there is an apparent fluctuation in the test section Mach number. This is considered to be more apparent than real inasmuch as

small errors in the static pressure readings introduce a large variation in the ratio of $\frac{p}{p_o}$ and hence in the computed Mach number. These traverses are tabulated in Figures 5.4 to 5.11.

5.4 Boundary Layer Correction Measurements

The experiments attempted in an effort to validate the theoretical boundary layer corrections to the nozzle contours were unsatisfactory. Although the results tabulated in Figure 5.12 indicate a trend in conformance with the theory used, they neither substantiate nor repudiate it. A more sophisticated and thorough exploration with perhaps a different approach is justified in this area.

5.5 Operation of Vacuum Pump and Quick-Acting Valve

The operation of the vacuum pump and the quick-acting valve are very satisfactory. The pump has the ability to evacuate the vacuum tank to an absolute pressure of less than 1.0mm of mercury. The quick-acting valve proved capable of holding the low vacuum vessel pressures to the extent that with the pump shut off, there was only a loss of 2.0mm of mercury over a period of fifteen minutes, beginning at an absolute pressure of 10mm of mercury.

5.6 Overall Evaluation

The overall evaluation of the University of Arizona 3" x 4.75" supersonic wind tunnel is that its operating characteristics are equally as good as those of tunnels utilizing fixed-geometry supersonic nozzles. The flow in the test section produced by its unique nozzle is relatively uniform at all Mach numbers, although the Mach number traverses based on static pressures do not adequately indicate this at the upper Mach numbers. Schlieren photographs have shown this to be true.

The simplicity and ease of operation of the tunnel are its primary assets. Since the side panels are removable, the tunnel can be changed from one testing configuration to another very quickly. This feature, coupled with the variable Mach number nozzle, makes it possible to conduct a wide range of experiments at various Mach numbers within a short period of time. For instance, during the experiments conducted to prepare this thesis, the nozzle setting was changed, all four side panels were loosened or removed, the instrumentation recalibrated and the next experiment prepared, all within a period of ten minutes.

Deficiencies found in the tunnel are few; the primary one being the discontinuity at the entrance to the diffuser. This is not considered a major drawback for the reasons previously mentioned.

This type facility is considered ideal for a university aerospace instructional program. The use of a continuously variable Mach number nozzle makes possible a relatively low cost, easily operated, extremely flexible supersonic wind tunnel that performs as well as those of more conventional but less sophisticated design.

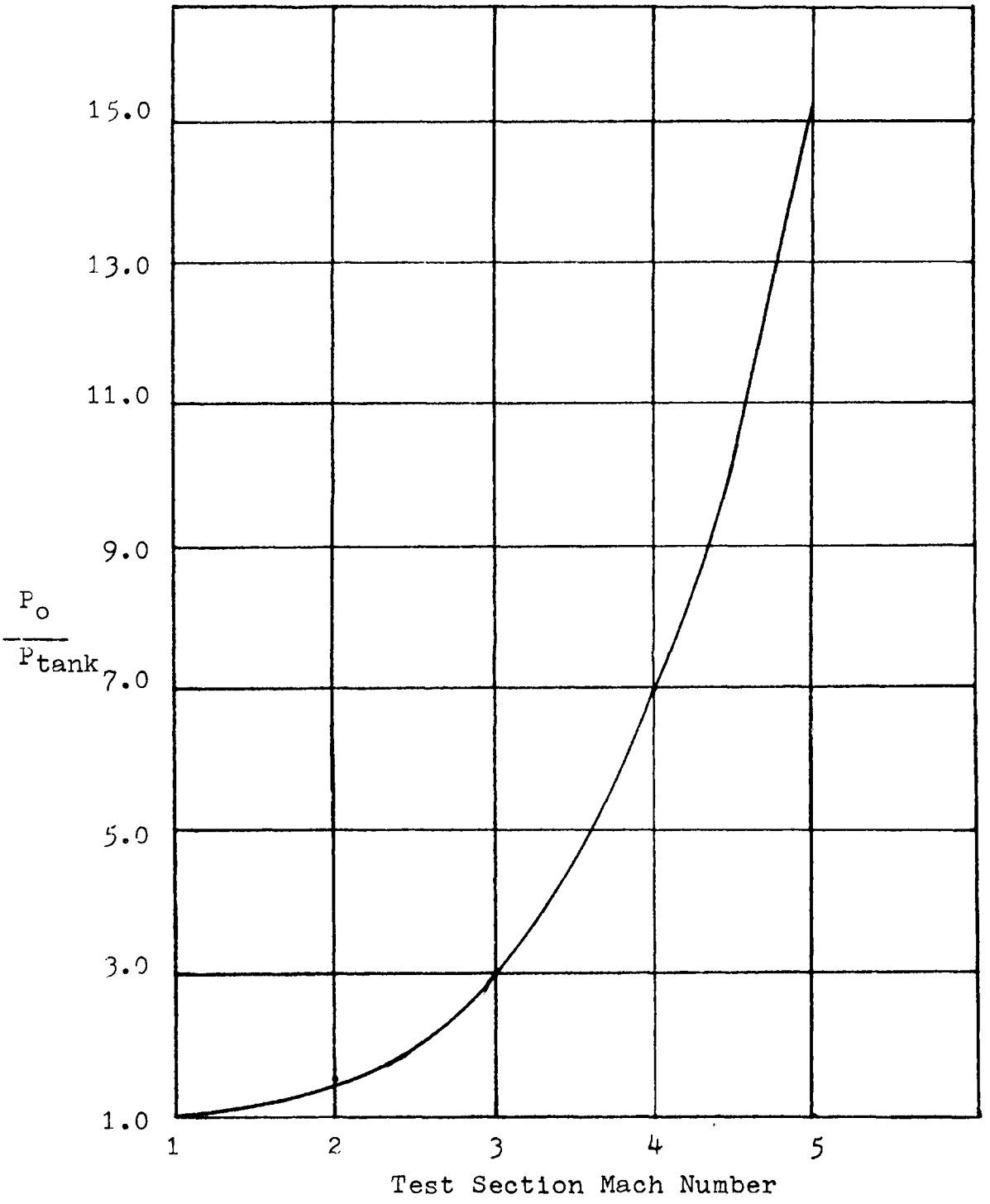

Figure 5.1 Minimum Pressure Ratio for Starting Tunnel Based on Normal Shock Recovery

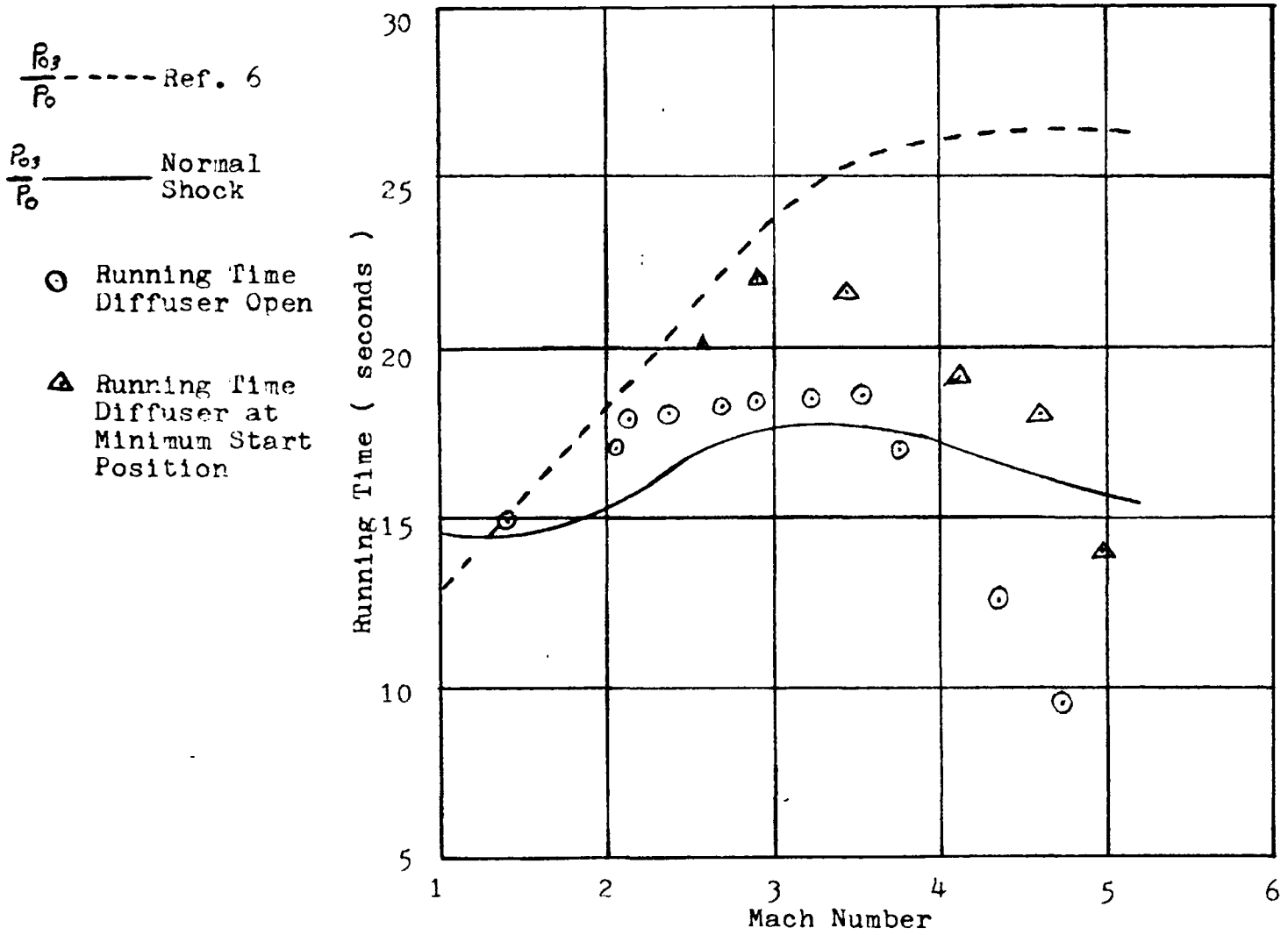

Figure 5.2 Wind Tunnel Running Time

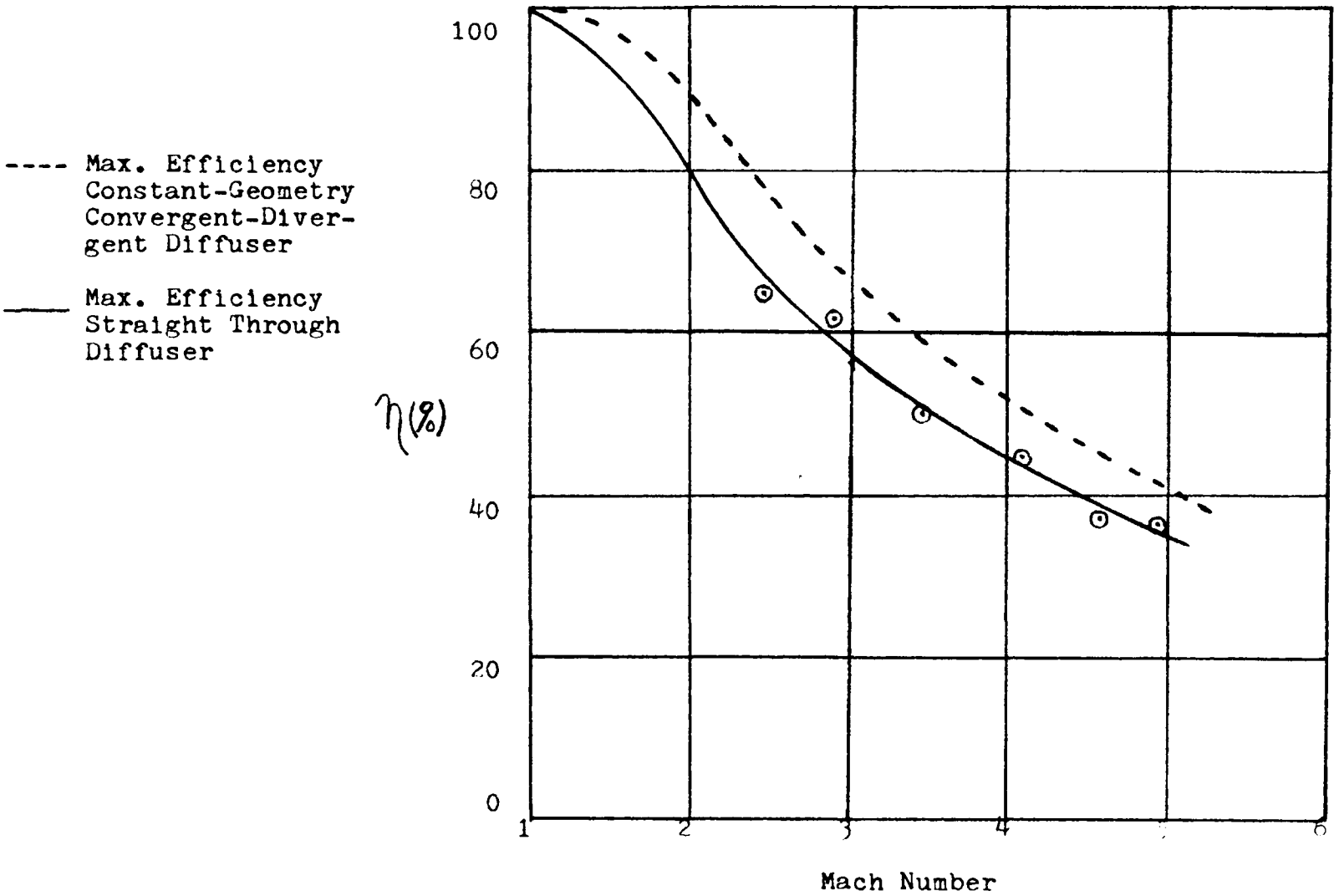

Figure 5.3 Diffuser Efficiency (η)

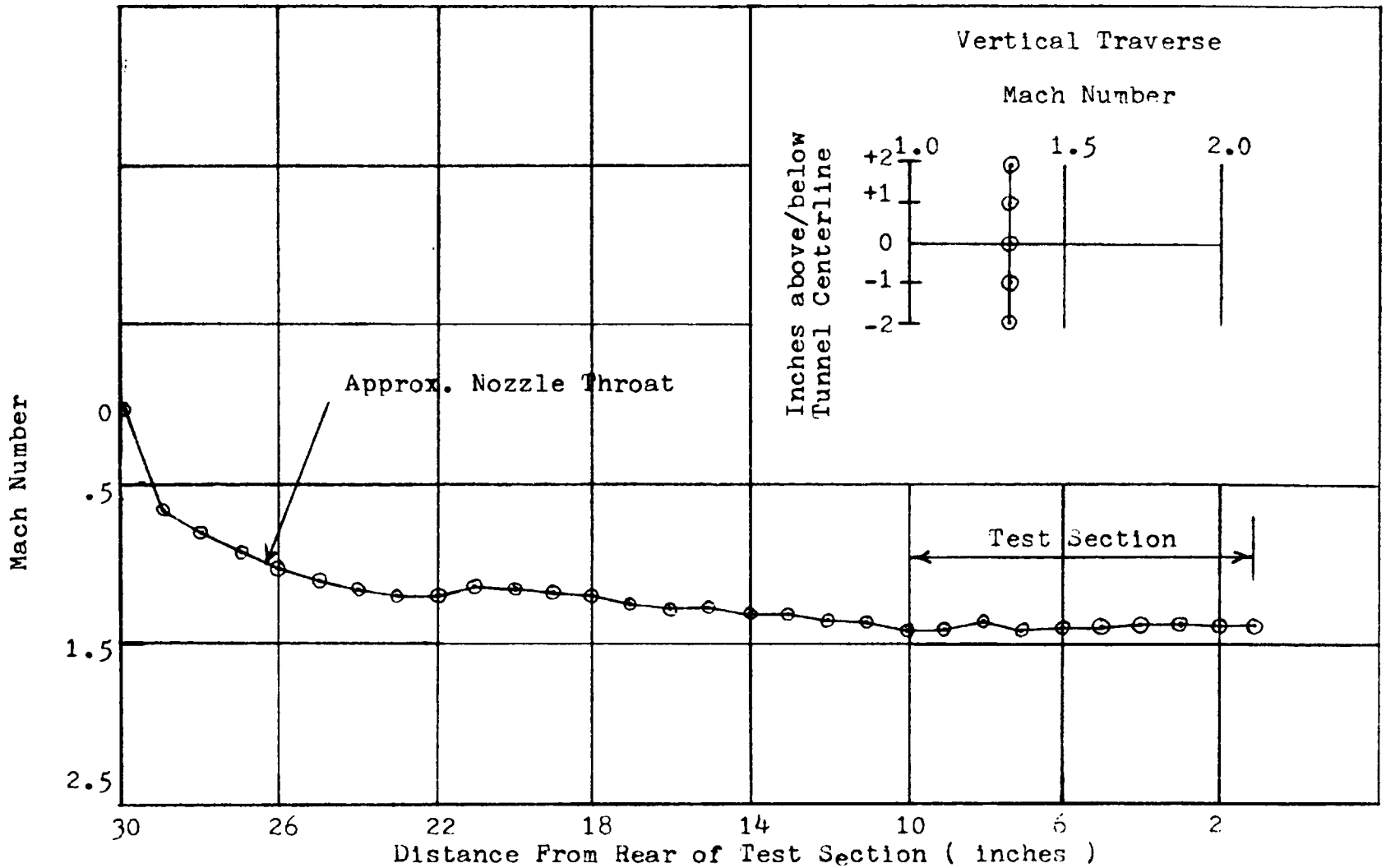

Figure 5.4 Centerline Mach Number Traverse, M = 1.39

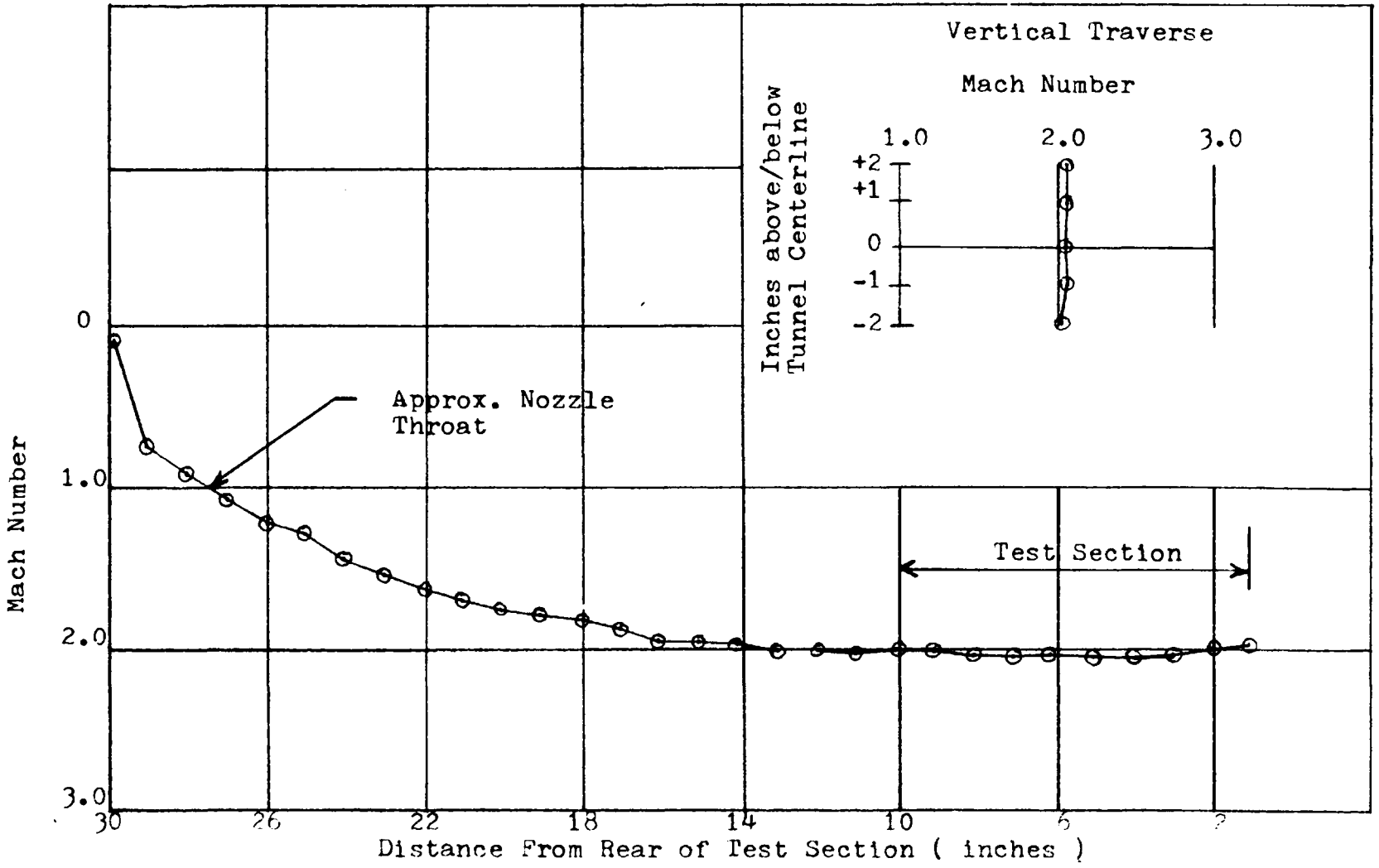

Figure 5.5 Centerline Mach Number Traverse, M = 2.05

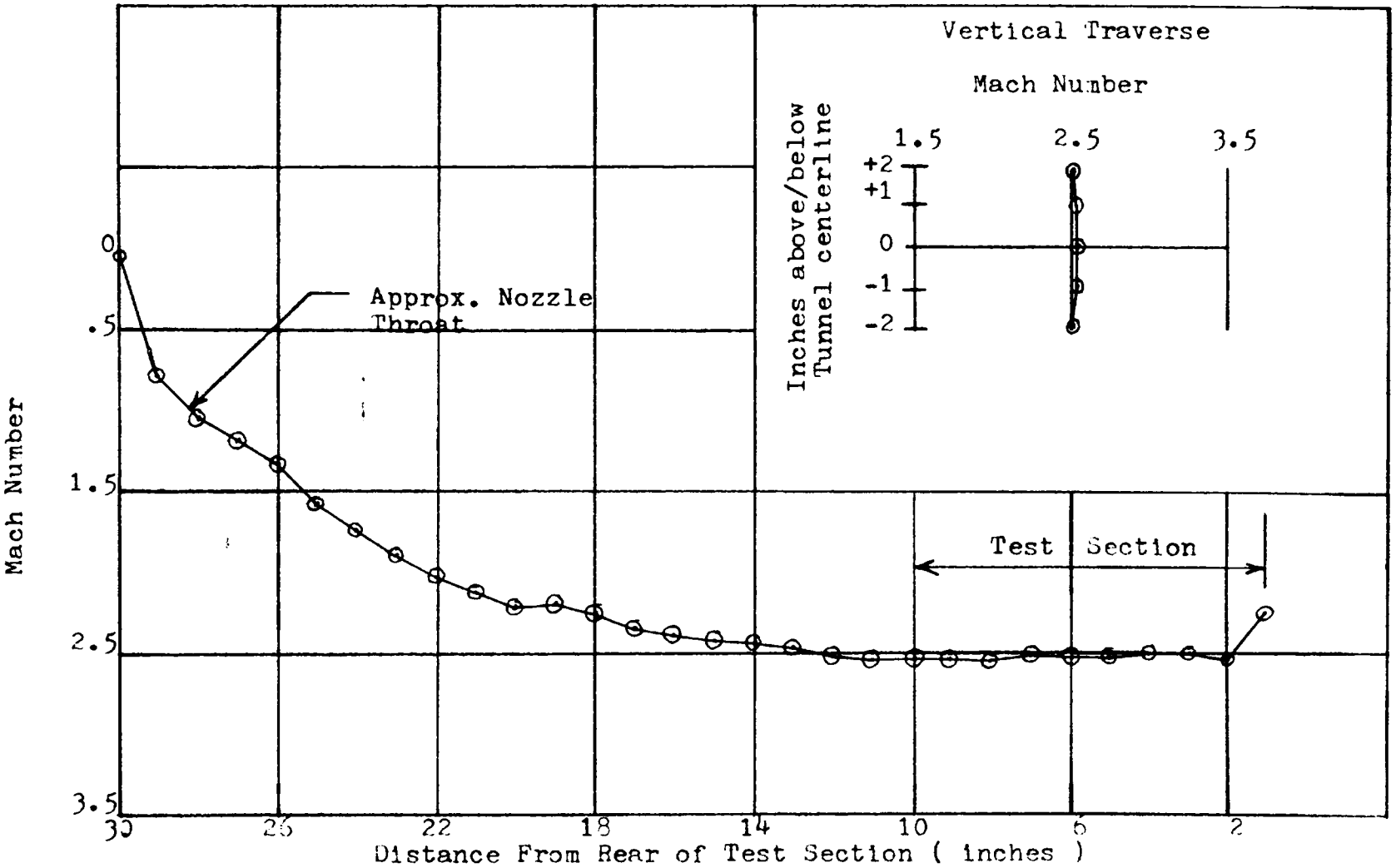

Figure 5.6 Centerline Mach Number Traverse, M = 2.56

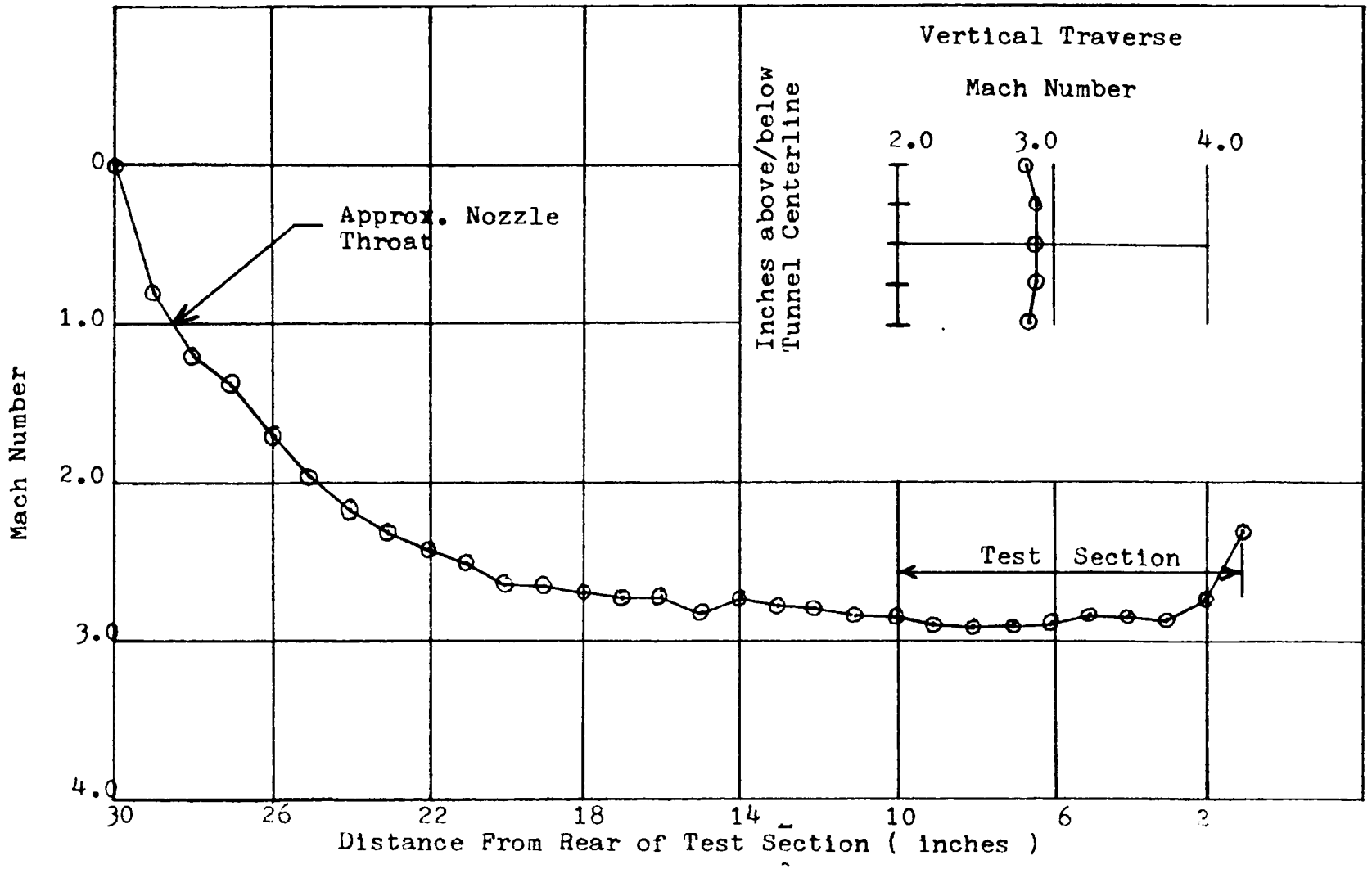

Figure 5.7 Centerline Mach Number Traverse, M = 2.87

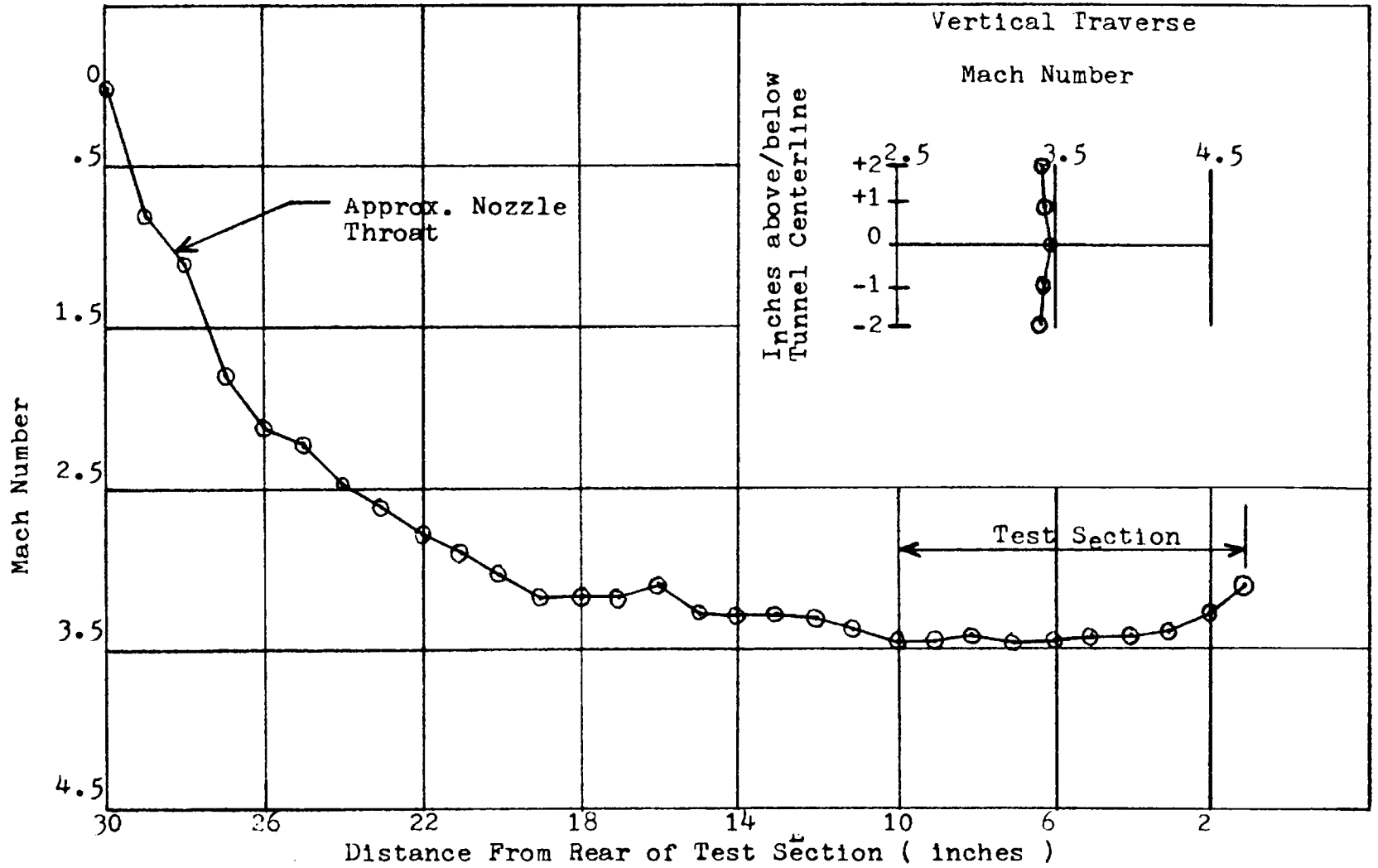

Figure 5.8 Centerline Mach Number Traverse, M = 3.46

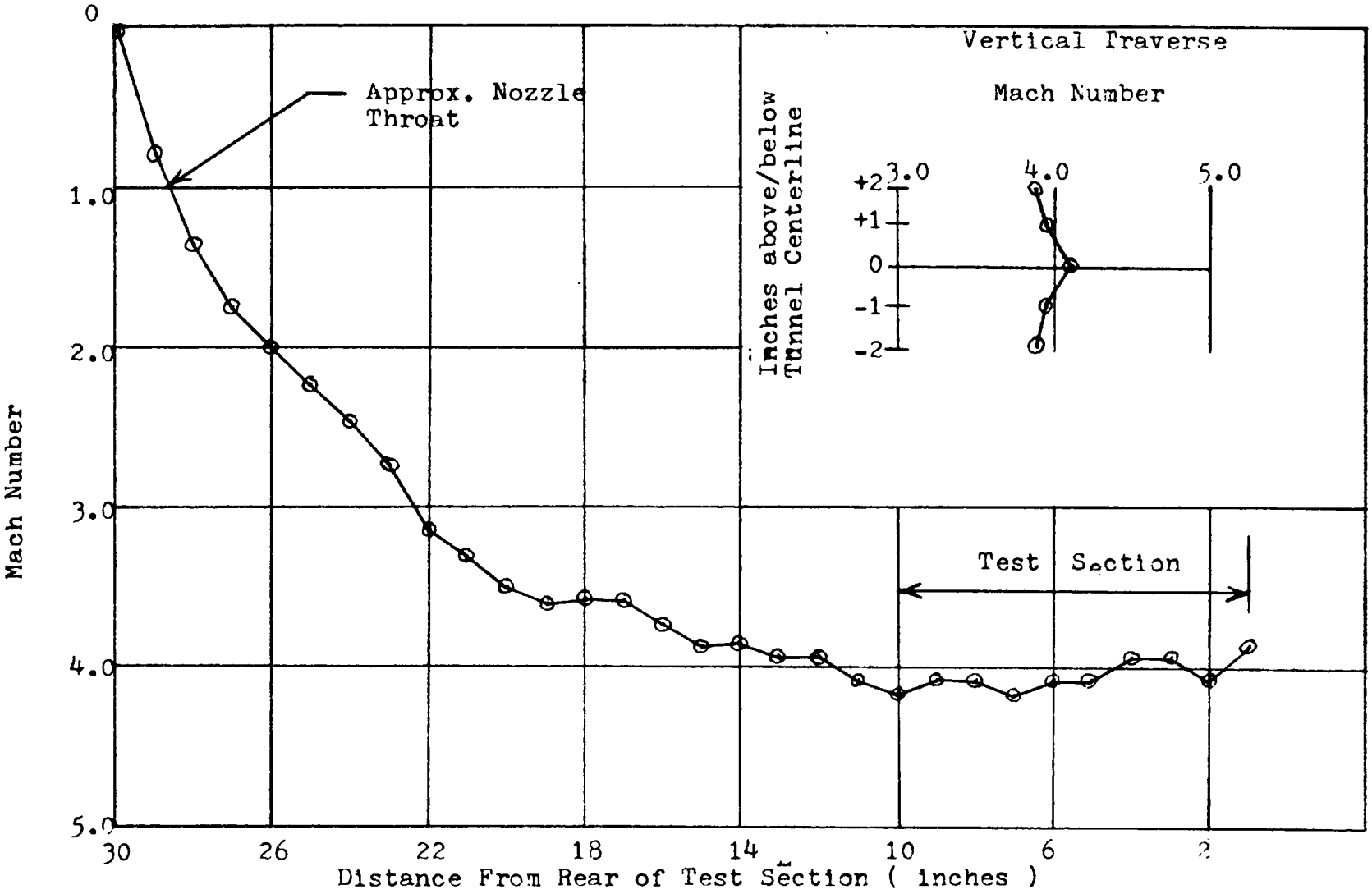

Figure 5.9 Centerline Mach Number Traverse, M = 4.10

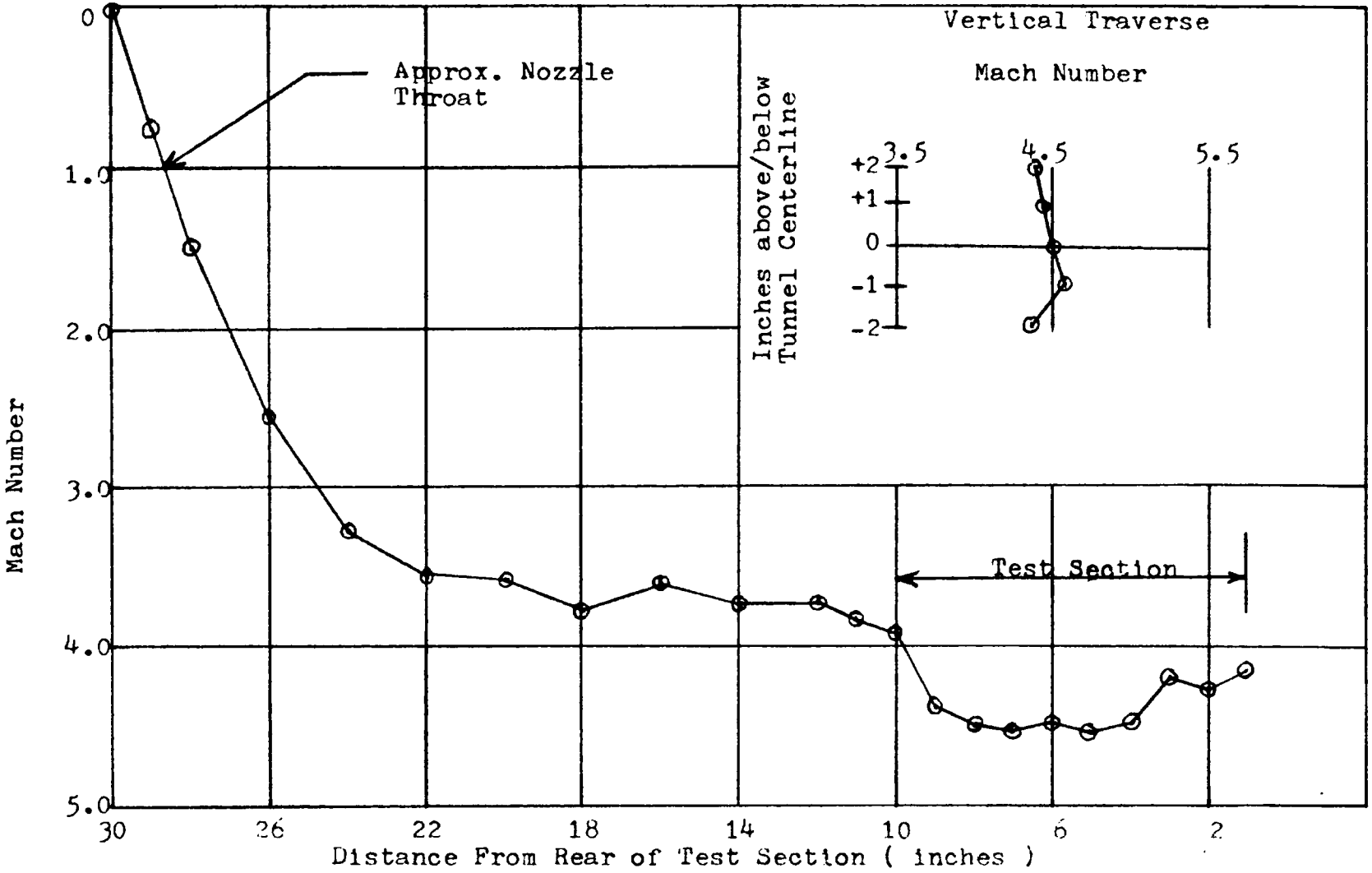

Figure 5.10 Centerline Mach Number Traverse, M = 4.57

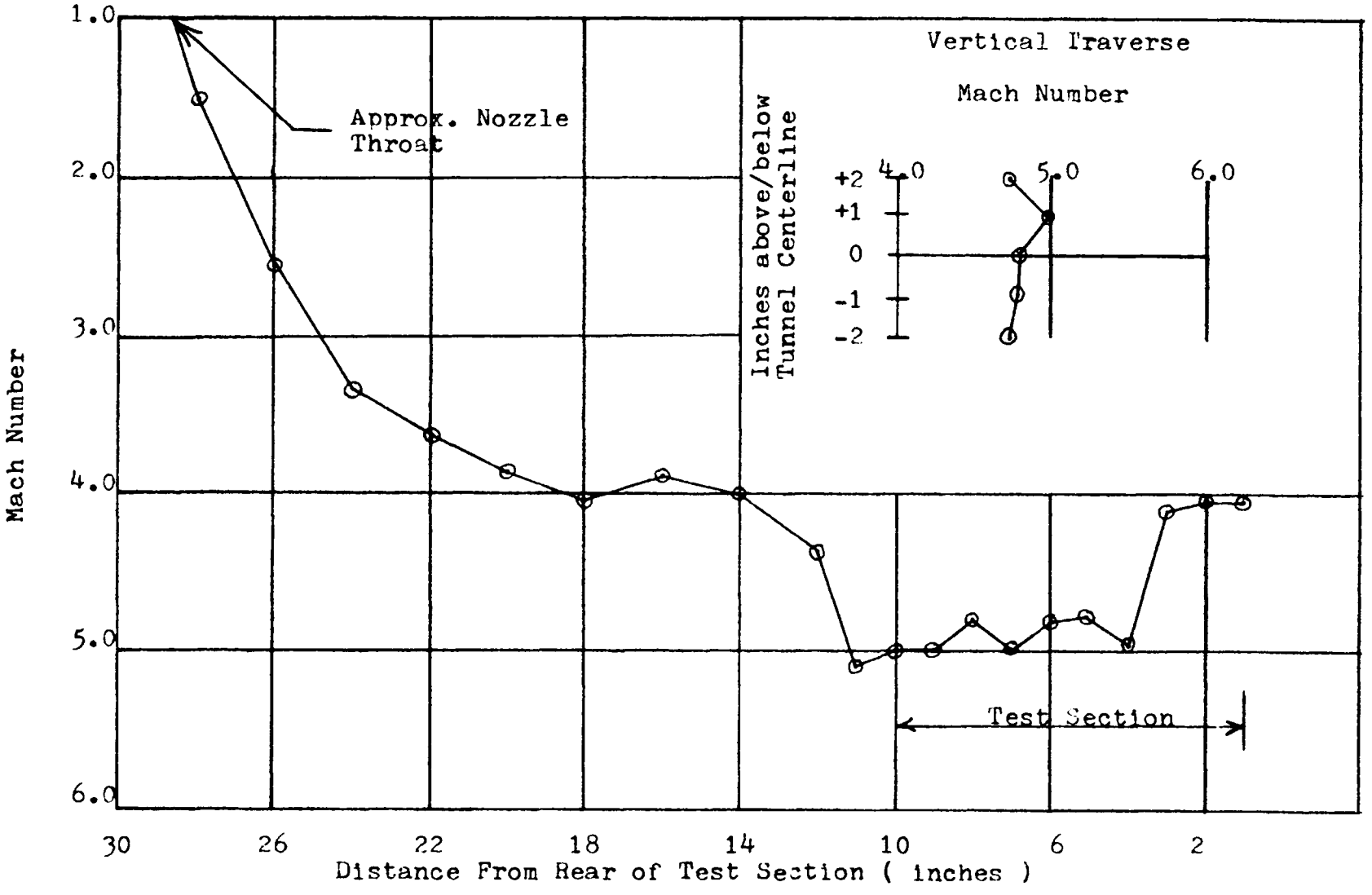

Figure 5.11 Centerline Mach Number Traverse, M = 4.99

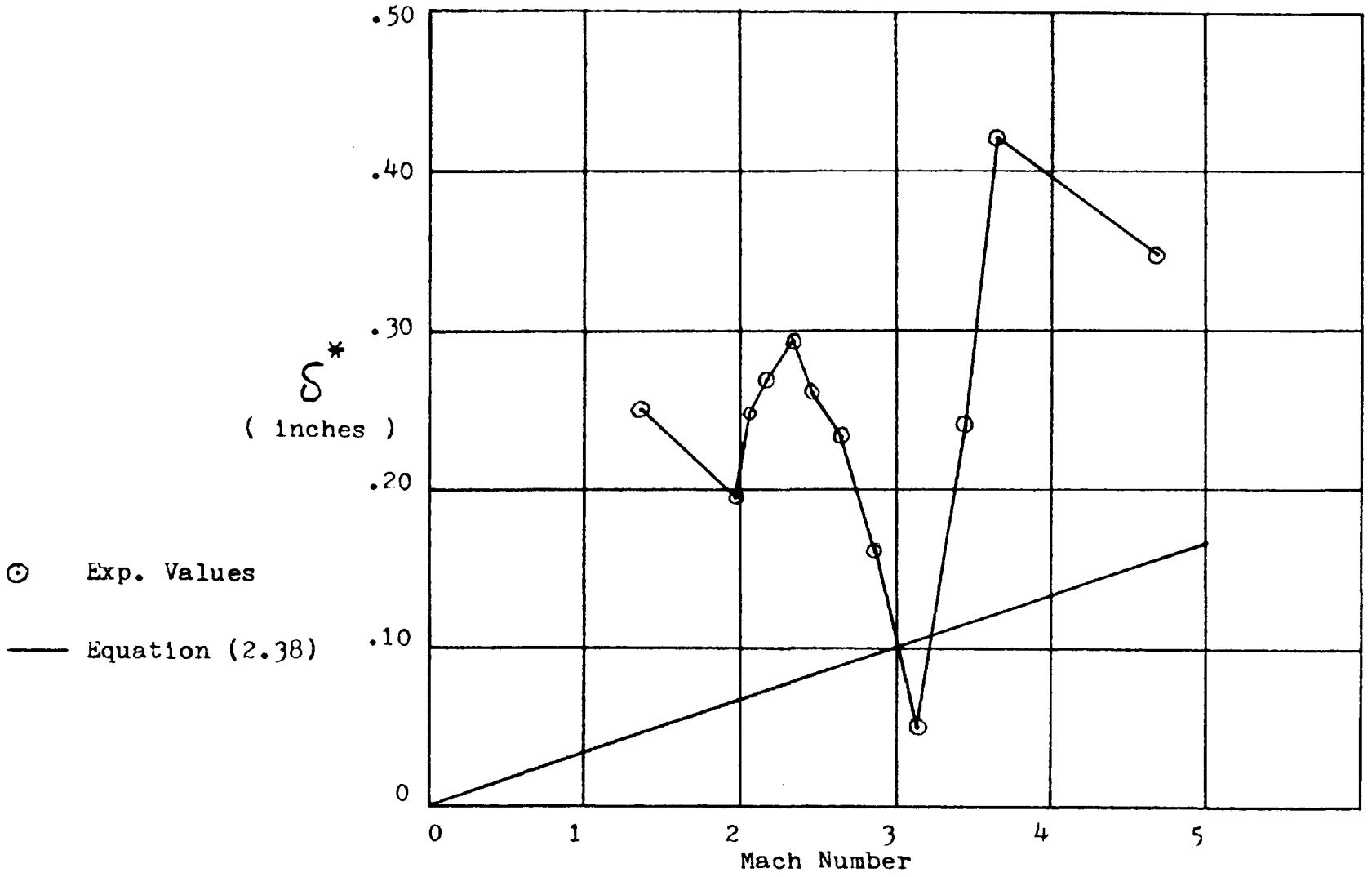

Figure 5.12 Boundary Layer Thickness in Test Section

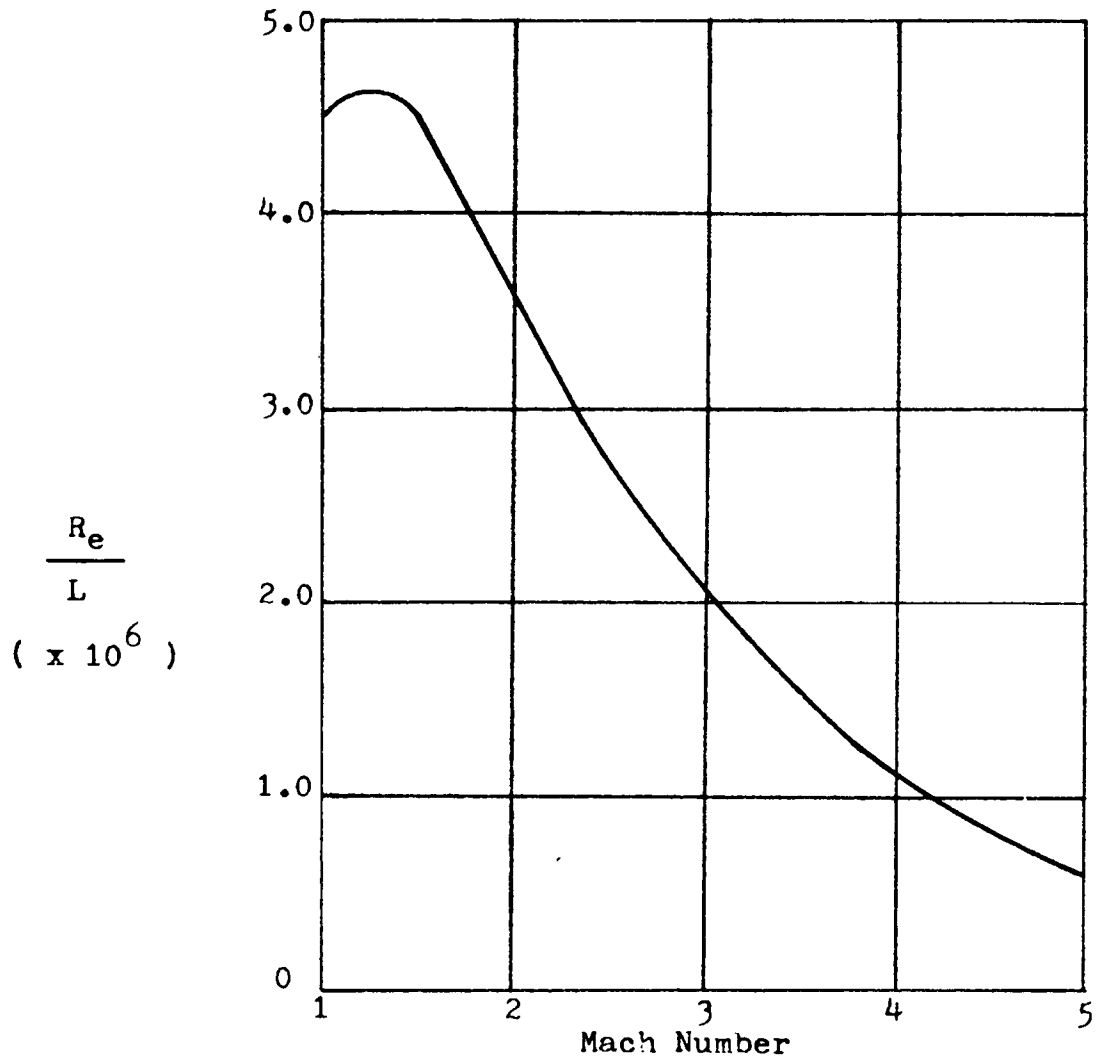

Figure 5.13 Test Section Reynolds' Number Per Foot

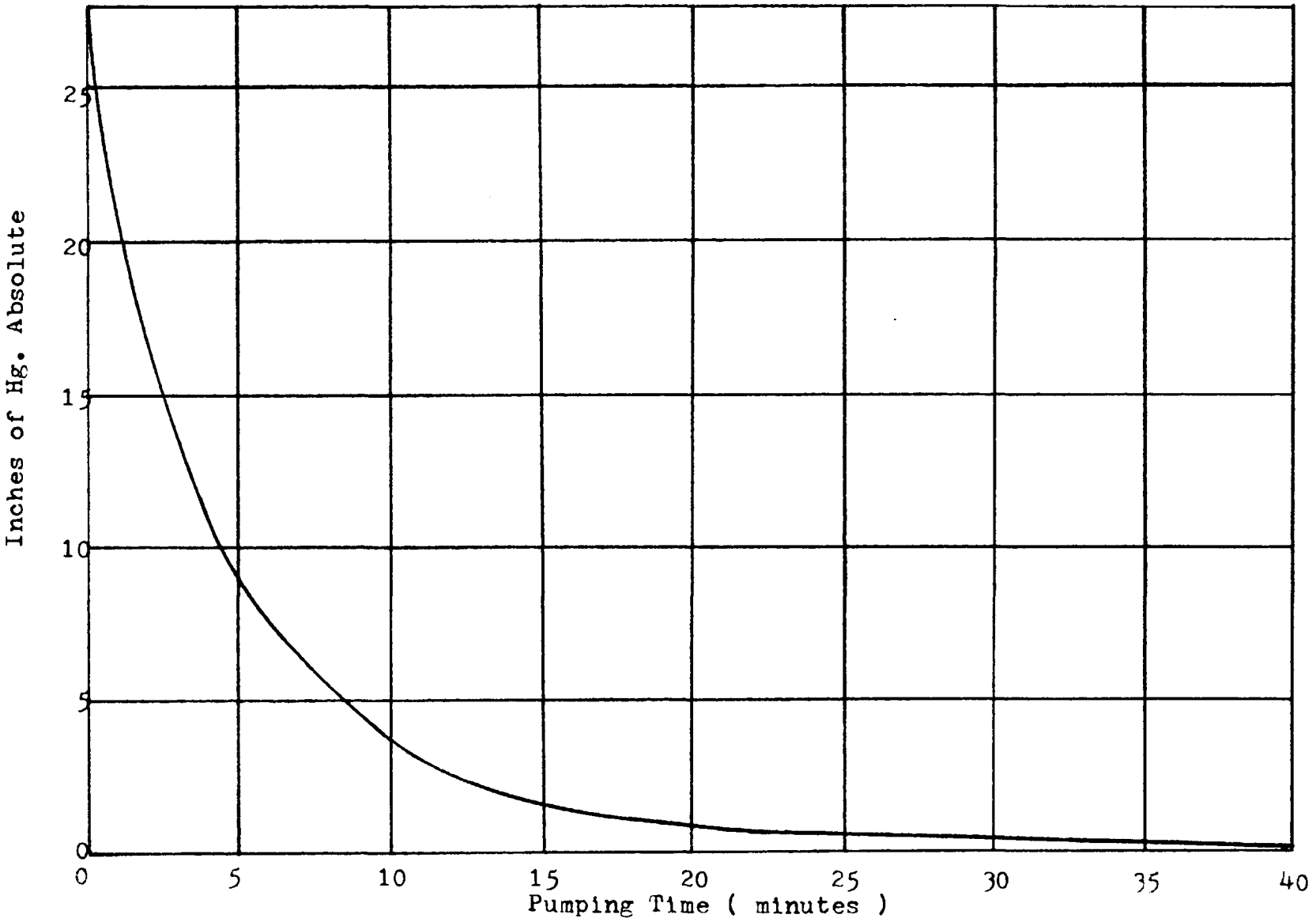

Figure 5.14 Vacuum Pump Performance

APPENDIX I

LIST OF SYMBOLS

A_1	Cross sectional area of test section.
a_o	Speed of sound at atmospheric conditions.
a_1	Speed of sound in test section.
c_p	Specific heat of air at constant pressure.
c_v	Specific heat of air at constant volume.
L	Distance in feet or inches.
M_1	Test section Mach number.
m	Mass of air.
$\dot{m}$	Mass flow rate.
p	Static pressure in tunnel.
p_i	Initial back pressure in vacuum tank.
p_o	Local atmospheric pressure.
p_{o3}	Stagnation pressure at diffuser exit.
p_f	Back pressure in vacuum tank at breakdown of supersonic flow.
R	Gas constant.
r	Temperature recovery factor.
R_e	Reynolds' number.
S	Sutherland's constant.
t_f	Tunnel running time.
T_1	Test section air temperature.
T_w	Adiabatic wall temperature.

u_1 Air velocity in test section.

V Volume of vacuum storage vessel.

x Distance from nozzle throat.

x_1 Distance from nozzle throat to test section.

γ Ratio of specific heats.

δ^* Displacement thickness of boundary layer.

Θ Momentum thickness of boundary layer.

ρ_0 Atmospheric air density.

ρ_1 Air density in test section.

ρ_w Wall air density.

ρ_i Initial air density in vacuum tank.

μ_0 Dynamic viscosity of atmospheric air.

μ_w Wall dynamic viscosity.

ν_w Wall kinematic viscosity.

LIST OF REFERENCES

1. Ames Research Staff, "Equations, Tables, and Charts for Compressible," N.A.C.A. Report 1135, Government Printing Office, Washington, D. C., 1953.

2. Fallis, W. B., Johnston, G. W., Lee, J. D., Tucker, N. B., and Wade, J. H., "Design and Calibration of the Institute of Aerophysics 16" x 16" Supersonic Wind Tunnel," U.T.I.A. Report No. 15, University of Toronto, Toronto, 1953.

3. Kwok, C. K. C., Construction and Calibration of the McGill University Supersonic Wind Tunnel, McGill University, Montreal, 1962.

4. Liepman, H. W. and Rosko, A., Elements of Gas Dynamics, Wiley and Sons, New York, 1957.

5. Ruptash, J. R., "Supersonic Wind Tunnel Theory, Design and Performance," U.T.I.A. Review No. 5, University of Toronto, Toronto, 1952.

6. Ruptash, J. R., "Boundary Layer Measurements in the U.T.I.A. 5 - by 7 - Inch Supersonic Wind Tunnel," U.T.I.A. Report No. 16, University of Toronto, Toronto, 1952.

7. Schlichting, Herman, Boundary Layer Theory, Translated by J. Kestin, McGraw Hill, New York, 1960.

8. Ruptash, J. R., "Growth of Boundary Layers in Supersonic Nozzles," Symposium on High Speed Aerodynamics, Summary of Proceedings, National Aeronautical Establishment, Ottawa, 1953.

9. The Theoretical Design of a Continuously-Variable Mach 5, Supersonic Wind Tunnel Nozzle, The Boeing Airplane Company, Wichita, 1957.

10. Glass, I. I., "The Calculation of Blast Time in an Intermittent Flow Type Wind Tunnel," U.T.I.A. Seminar, University of Toronto, Toronto, 1950.